

Statistical mechanics of logarithmic REM: duality, freezing and extreme value statistics of $1/f$ noises generated by Gaussian free fields

This article has been downloaded from IOPscience. Please scroll down to see the full text article.

J. Stat. Mech. (2009) P10005

(<http://iopscience.iop.org/1742-5468/2009/10/P10005>)

View [the table of contents for this issue](#), or go to the [journal homepage](#) for more

Download details:

IP Address: 129.175.97.14

The article was downloaded on 20/09/2010 at 15:40

Please note that [terms and conditions apply](#).

Statistical mechanics of logarithmic REM: duality, freezing and extreme value statistics of $1/f$ noises generated by Gaussian free fields

Yan V Fyodorov¹, Pierre Le Doussal² and Alberto Rosso³

¹ School of Mathematical Sciences, University of Nottingham, Nottingham NG7 2RD, UK

² CNRS-Laboratoire de Physique Théorique de l'Ecole Normale Supérieure, 24 rue Lhomond, 75231 Paris, Cedex, France⁴

³ Laboratoire de Physique Théorique et Modèles Statistiques, CNRS (UMR 8626), Université Paris-Sud, Bâtiment 100, 91405 Orsay Cedex, France
E-mail: Yan.Fyodorov@nottingham.ac.uk, ledou@lpt.ens.fr and rosso@lptms.u-psud.fr

Received 14 July 2009

Accepted 15 September 2009

Published 7 October 2009

Online at stacks.iop.org/JSTAT/2009/P10005

[doi:10.1088/1742-5468/2009/10/P10005](https://doi.org/10.1088/1742-5468/2009/10/P10005)

Abstract. We compute the distribution of the partition functions for a class of one-dimensional random energy models with logarithmically correlated random potential, above and at the glass transition temperature. The random potential sequences represent various versions of the $1/f$ noise generated by sampling the two-dimensional Gaussian free field (2D GFF) along various planar curves. Our method extends the recent analysis of Fyodorov and Bouchaud (2008 *J. Phys. A: Math. Theor.* **41** 372001) from the circular case to an interval and is based on an analytical continuation of the Selberg integral. In particular, we unveil a *duality relation* satisfied by the suitable generating function of free energy cumulants in the high temperature phase. It reinforces the freezing scenario hypothesis for that generating function, from which we derive the distribution of extrema for the 2D GFF on the $[0, 1]$ interval. We provide numerical checks of the circular case and the interval case and discuss universality and various extensions. The relevance to the distribution of the length of a segment in Liouville quantum gravity is noted.

⁴ LPTENS is a Unité Propre du CNRS associée à l'Ecole Normale Supérieure et à l'Université Paris Sud.

Keywords: conformal field theory (theory), self-affine roughness (theory), disordered systems (theory), stochastic processes

ArXiv ePrint: [0907.2359](https://arxiv.org/abs/0907.2359)

Contents

1. Introduction	3
2. The model and moments	5
2.1. The interval model	5
2.2. Positive moments	6
2.3. Negative moments	6
2.4. From moments to distribution: the circular case and duality in the high temperature phase	7
2.5. From moments to distribution: generalities	8
3. Analytical continuation at the critical temperature and distribution of minima on the interval	9
3.1. No edge charges	9
3.2. Extension to edge charges; the binding transition	11
4. The high temperature phase for the $[0, 1]$ interval with no end charges	13
5. The Gaussian weight model	14
6. Numerical study	15
6.1. The circular ensemble	15
6.2. Universality of the circular ensemble: cyclic matrices, and s GFF inside a disk with a Dirichlet boundary condition	17
6.2.1. A GFF along an arbitrary circle.	19
6.2.2. Other periodic models.	20
6.3. The interval	21
6.4. Temperature dependence of the second cumulant of the free energy	23
6.5. More open questions on universality	23
7. Conclusion	24
Acknowledgments	26
Appendix A. The special case of $[0, 1]_{-1/2, -1/2}$	26
Appendix B. Some properties of the generalized Barnes function	27
Appendix C. High temperature expansions	28
C.1. High temperature expansion of REM models	28
C.2. High temperature expansion of the analytical result for the interval	31
References	32

J. Stat. Mech. (2009) P10005

1. Introduction

Describing the detailed statistics of the extrema of M random variables V_i with logarithmic correlation built from those of the two-dimensional Gaussian free field (2D GFF) $V(x)$ is a hard and still mostly open problem. It arises in many fields from physics and mathematics to finance. The 2D GFF is a fundamental object intimately related to conformal field theory [1], and being also a building block of the Liouville random measures $e^{V(z,\bar{z})}dzd\bar{z}$, attracted much interest in high energy physics, quantum gravity, and pure mathematics communities; see [2] for an extensive list of references. In the context of condensed matter physics the 2D GFF is of interest for describing e.g. fluctuating interfaces between phases [3], e.g. their confinement properties, multi-fractal properties of wavefunctions of Dirac particles in random magnetic fields [4] and associated Boltzmann–Gibbs measures [5], glass transitions of random energy models with logarithmic correlated energies [6], 2D self-gravitating systems [7] etc. Descriptions of the level lines of the GFF such as Schramm–Loewner evolutions (SLE) and conjectured relations to the welding problem [8] have also contributed to a revival of interest in the statistics of the GFF. In mathematical finance there is a strong current interest in limit log-normal multi-fractal processes [9] (also called log-infinitely divisible multi-fractal random measures), which is just a closely related incarnation of the same object; see e.g. [10, 11]. Last but not least important is looking at the logarithmically correlated random sequences such as those representing various instances of $1/f$ noises; see e.g. [12] and [13]. Such noises regularly appear in many applications, and were recently discussed in the context of quantum chaos, where logarithmic correlations arise in sequences of energy levels [14] or, as one can surmise, in the zeros of the zeta Riemann function. All of this makes understanding extreme value statistics of such noises an interesting and important problem.

While the leading behavior $V_{\min} \sim -2A \ln M$ is rigorously proved [15], surprisingly little knowledge exists on finer properties of the statistics of the GFF-related minima, even heuristically. To serve to remedy this as well as for many other purposes it is of great interest to study the canonical partition function $Z(\beta) = \sum_{i=1}^M e^{-\beta V_i}$ for the corresponding random energy model (REM) as a function of the inverse temperature $\beta = 1/T$. The distribution $P(F)$ of the free energy $F = -T \ln Z$ reduces in the limit of zero temperature $T = 0$ to the distribution of the minimum V_{\min} . A few instances of REMs can be solved explicitly, and are frequently useful as approximations: (i) uncorrelated energies with variance $\sim \ln M$, i.e. Derrida’s original REM [16], which gives the correct constant A [4]; (ii) paths with random weights on trees, whose energies exhibit a similar logarithmic scaling of correlations, but with a hierarchical structure rather than a translationally invariant one [17, 18]; (iii) the infinite-dimensional Euclidean version of the logarithmically correlated REM and its further ramifications [5, 19]. In particular, the close analogy of GFF-related statistical mechanics with the models on trees [4, 6], also noted in probability theory [15], arises naturally in an approximate, i.e. one-loop, RG method, and led to the conjecture [6] that

$$V_{\min} = a_M + b_M y \quad (1)$$

with

$$a_M = A(-2 \ln M + \tilde{\gamma} \ln \ln M + O(1)), \quad b_M = A + O(1/\ln(M)) \quad (2)$$

where $\tilde{\gamma} = 3/2$ and y is a random variable of order unity whose probability density has universal tails $p(y) \sim |y|e^y$ on the side $y \rightarrow -\infty$. In addition it was convincingly demonstrated that the log-correlated REM exhibits a freezing transition to a glass phase dominated by a few minima, at the same T_c as predicted by (i) and (ii) [6, 19]. An outstanding problem left fully open was that of characterizing the shape of the distribution of the minimum beyond the tail, and in particular investigating whether the universality also extends to that regime.

To address this issue, Fyodorov and Bouchaud [13] (FB) recently considered a particular circular-log variant of the REM. Denoting here and henceforth the averaging over the random potential with the overbar, the circular-log model is defined via the correlation matrix $C_{ij} = \overline{V_i V_j}$ identical to those of M equidistant points $z_j = \exp(i(2\pi j/M))$ on a circle $C_{jk} = 2G(z_j - z_k)$, where $G(z - z') = -\ln|z - z'|$ is the full plane Green function of the 2D GFF. Equivalently, the above covariance function represents a 2π -periodic real-valued Gaussian random process $V(x) = \sum_{l=1}^{\infty} (v_l e^{ilx} + \bar{v}_l e^{-ilx})$ with a *self-similar* spectrum $\langle v_l \bar{v}_m \rangle = l^{-(2H+1)} \delta_{lm}$ characterized by the particular choice of the Hurst exponent $H = 0$. Such a process therefore represents a version of the so-called $1/f$ noise.

From the moments $\overline{Z^n}$ FB reconstructed the distribution $P(Z)$ above and at T_c . From such a point they proceeded by assuming that for such a model the same freezing scenario as found in [6] holds so that the generating function

$$g_\beta(y) = \overline{\exp(-e^{\beta y} Z / Z_e)}, \quad Z_e = M^{1+\beta^2} / \Gamma(1 - \beta^2) \quad (3)$$

remains in the thermodynamic limit $M \gg 1$ *temperature independent* everywhere in the glass phase $T \leq T_c$. As a result of such a conjecture they arrived at the distribution of the minimum of the random potential in their problem. The corresponding probability density for the variable y (defined in (1) with $A = 1$) turned out to be given by $p(y) = -g'_\infty(y)$ where

$$g_\infty(y) = g_{\beta_c}(y) = 2e^{y/2} K_1(2e^{y/2}). \quad (4)$$

Such a density does indeed exhibit the universal Carpentier–Le Doussal tail $p(y \rightarrow -\infty) \sim -ye^y$.

Our broad aim is to investigate analytically and numerically the validity and universality of the above result, and to extend it to other models with logarithmic correlations. In pursuing this goal we will be able, in particular, to extract statistics of the extrema of the (full plane) GFF sampled along an interval, $[0, 1]$, with eventually some charges at the endpoints of the interval. This breaks the circular symmetry of the correlation matrix and one finds a different distribution. The moments $\overline{Z^n}$ turn out to be given in some range of positive integer n by the celebrated Selberg integrals [20]⁵ and a first (non-trivial) task is to analytically continue them to arbitrary n . After suggesting a certain method for such a continuation we are able to deduce the distribution of free energy $P(F)$ and $g_\beta(y)$ at the freezing temperature $\beta = \beta_c$. The same conjecture as in FB then yields the distribution of the minimum. As a by-product of our method we reveal a remarkable *duality property* enjoyed in the high temperature phase by the generating function precisely defined as in (3) and unnoticed in [13]. We conjecture such a duality

⁵ In a somewhat different but related context this fact was noticed, but not much exploited; see [9].

to be intimately related to the mechanisms behind the freezing phenomenon. Finally we use direct numerical simulations to verify the freezing scenario for the circular ensemble and the resulting distribution (4), as well as to test the new results of this paper for the interval case. Universality and other cases are discussed at the end.

2. The model and moments

2.1. The interval model

Our starting point is the following continuum version of the partition function of the random energy model generated by a Gaussian-distributed logarithmically correlated random potential $V(x)$ defined on the interval $[0, 1]$:

$$Z = \epsilon^{\beta^2} \int_0^1 dx x^a (1-x)^b e^{-\beta V(x)} \quad (5)$$

with $a, b > -1$ real numbers and $\beta > 0$. The potential $V(x)$ is considered to have zero mean and covariance inherited from the two-dimensional GFF:

$$\overline{V(x)V(x')} = C(x-x') = -2 \ln |x-x'|. \quad (6)$$

For the integral (5) to be well defined one needs to define a short scale cutoff $\epsilon \ll 1$. We therefore tacitly assume in the expression (6) $V \rightarrow V_\epsilon$, with the regularized potential being also Gaussian with a covariance function $C_\epsilon(x-x')$, such that the variance is $C_\epsilon(0) = 2 \ln(1/\epsilon)$. We put for convenience the factor ϵ^{β^2} in front of the integral to ensure that the integer moments $\overline{Z^n}$ are independent of ϵ in the high temperature phase; see equation (7) below. At this stage we do not need to specify the ϵ -regularized form⁶, but it is convenient for our purposes below to require that $C_\epsilon(x) = C(x)$ for $|x| > \epsilon$. Note that for $a = b = 0$ the Gibbs measure of the disordered system becomes identical to the random Liouville measure, and that Z can be interpreted as the (fluctuating) length of a segment in Liouville quantum gravity; see e.g. [2].

Below we will also consider a grid of M points x_i , uniformly spaced w.r.t. the length element $dl = dx x^a (1-x)^b$ and the set of values $V_i = V(x_i)$, $i = 1, \dots, M$. The elements of the correlation matrix $\overline{V_i V_j} = C_{ij}$ at these grid values are $C_{ij} = -2 \ln(|i-j|/M)$ for $i \neq j$, and $C_{ii} = 2 \ln M + W$ where $W = \ln(1/(\epsilon M))$ is a constant of order unity, and we will be interested in the limit⁷ of large M at fixed ϵM . This generalizes the grid on the unit circle studied in [13] where $x_j = e^{i\theta_j}$ with $\theta_j = 2\pi j/M$ and $C_{ij} = C(x_i - x_j) = -\ln |\sin \frac{\theta_i - \theta_j}{2}|$. We will compare below the two situations. In each case one defines the corresponding (discretized) REM using the partition function $Z_M = \sum_{i=1}^M e^{-\beta V_i}$. We expect, as shown in [13] and discussed below, that there is a sense in which universal features of the discretized version can be described in terms of those of the continuum one in the large M limit.

⁶ There are various useful cutoffs, e.g. the circle average (see e.g. [2]) or the scale invariant cone construction (see e.g. [10]).

⁷ In practice we want to have $\min_i (|x_i - x_{i+1}|) > \epsilon$.

2.2. Positive moments

Let us now compute the positive integer moments of Z . Defining $\gamma = \beta^2$, a straightforward calculation gives

$$\overline{Z^n} = \int_0^1 \cdots \int_0^1 \prod_{i=1}^n dx_i x_i^a (1-x_i)^b \prod_{1 \leq i < j \leq n} \frac{1}{|x_i - x_j|^{2\gamma}} \quad (7)$$

where the small scale cutoff is implicit and modifies the expressions for $|x_i - x_j| < \epsilon$. For a fixed $n = 1, 2, \dots$, a well defined and universal $\epsilon \rightarrow 0$ limit exists whenever the integral (7) is convergent, in which case it is given by the famous Selberg integral formula [20] $\overline{Z^n} = s_n$, with

$$s_n(\gamma, a, b) = \prod_{j=1}^{j=n} \frac{\Gamma[1+a-(j-1)\gamma]\Gamma[1+b-(j-1)\gamma]\Gamma(1-j\gamma)}{\Gamma[2+a+b-(n+j-2)\gamma]\Gamma(1-\gamma)} \quad (8)$$

where $\Gamma(x)$ is the Euler gamma function. For $a, b > 0$ the domain of convergence is given by $\gamma < 1/n$. It corresponds to the well known fact that for continuum REM models the distribution of $P(Z)$ develops algebraic tails⁸; hence integer moments $\overline{Z^n}$ become infinite at a series of transition temperatures $T_c^{(n)} = \sqrt{n}$. The true transition in the full Gibbs measure happens however only at $T_c = 1$, i.e. $\gamma = \gamma_c = 1$. Above T_c the distribution $P(Z)$ exists in the limit $\epsilon = 0$, while the formally divergent moments start depending on the cutoff parameter ϵ . An analogous result arises in the circular-log ensemble [13] where the moments of Z_M were analyzed, as recalled below. The generalizations for complex a, b, β , which connect to sine-Gordon physics, as well as a detailed study of the competition with binding transitions to the edges for $a, b < -1$ (in the presence of a cutoff), are mostly left for future studies, although some remarks about the binding transitions are made below in section 3.2⁹.

2.3. Negative moments

Our first aim is to reconstruct the distribution $P(Z)$ from its moments in the high temperature phase $\gamma \leq 1$. This entails analytical continuation of the Selberg integral which is a well known difficult problem. Here we present a solution of this problem at T_c , the most interesting point. Let us first obtain the negative integer moments for any $T \geq T_c$. It is convenient to define

$$z = \Gamma(1-\gamma)Z = e^{-\beta f}, \quad z_n = \overline{z^n} \quad (9)$$

which, as found below, and in [13], has a well defined limit as $T \rightarrow T_c^+$. One then checks for $a = b = 0$ the following recursion relation:

$$\frac{z_n}{z_{n-1}} = \frac{\Gamma[1-n\gamma]\Gamma^2[1-(n-1)\gamma]\Gamma[2-(n-2)\gamma]}{\Gamma[2-(2n-3)\gamma]\Gamma[2-(2n-2)\gamma]} \quad (10)$$

with $z_1 = \Gamma(1-\gamma)$ (which also implies $z_0 = 1$), and a similar formula for any a, b . Let us now perform the formal analytic continuation to negative integer moments $m_k \equiv z_{-k}$

⁸ For finite grid $1/M$ these tails are cut far away by log-normal behavior; see a detailed discussion in [13].

⁹ The full conditions for convergence in (8) are $\Re(a), \Re(b) > -1$, $\Re(\gamma) < \min(1/n, (a+1)/(n-1), (b+1)/(n-1))$.

in the above recursion (10) as $m_k/m_{k+1} \equiv z_n/z_{n-1}|_{n \rightarrow -k}$. It is then easy to solve the recursion starting from $m_0 = z_0 = 1$. Restoring a, b we find

$$z_{-k} = \prod_{j=1}^k \frac{\Gamma[2 + a + b + (k + j + 1)\gamma]}{\Gamma[1 + (j - 1)\gamma] \Gamma[1 + a + j\gamma] \Gamma[1 + b + j\gamma]}. \tag{11}$$

We have checked that these expressions satisfy the convexity property $z_n^{p-m} z_p^{m-n} \geq z_m^{p-n}$ for any integers $n < m < p$ of arbitrary sign, which is a necessary condition for positivity of a probability. For $a = b = 0$ the formula (11) was announced very recently in [11] as a rigorous consequence of certain recursion relations for Selberg integrals.

Note that the domain in a, b where (11) remains well defined extends to $a > -1 - \gamma$, $b > -1 - \gamma$, a region larger than the naive expectation $a, b > -1$. This is a signature of the competition between binding to the edge and the random potential as discussed below.

2.4. From moments to distribution: the circular case and duality in the high temperature phase

Let us recall for comparison the corresponding analysis for the circle [13]. There, the corresponding Dyson Coulomb gas integrals give $z_n = \Gamma(1 - n\gamma)$, and such a simple formula admits the natural continuation to negative moments $n = -k$. This allows to immediately and uniquely identify the distribution of $1/z$ and leads to the probability densities:

$$P(z) = \beta^{-2} z^{-1/\beta^2 - 1} \exp(-z^{-1/\beta^2}), \quad \tilde{P}(f) = \beta^{-1} \exp(f/\beta - e^{f/\beta}). \tag{12}$$

The latter formula implies that the free energy is distributed with a Gumbel probability density for all $T \geq T_c$. Alternatively the (formal) series for positive moments $g_\beta(y) := \overline{e^{-ze^{\beta y}}} = \sum_{n=0}^\infty ((-1)^n/n!) z_n e^{n\beta y}$ is directly summed using $\Gamma(z) = \int_0^\infty e^{-t} t^{z-1} dt$ into the following generating function:

$$g_\beta(y) = \int_0^\infty dt \exp\{-t - e^{\beta y} t^{-\beta^2}\}. \tag{13}$$

What went unnoticed in [13] was the remarkable duality relation satisfied by the exact expression for this function¹⁰:

$$g_\beta(y) = g_{1/\beta}(y). \tag{14}$$

To see this directly define $\tau = e^{\beta y} t^{-\beta^2}$ implying $t = \tau^{-(1/\beta^2)} e^{-y/\beta}$, and after substituting this back to the integral (13) we see that

$$g_\beta(y) = -\frac{1}{\beta^2} \int_0^\infty d\tau \tau^{-1-(1/\beta^2)} e^{y/\beta} \exp\{-\tau - e^{y/\beta} \tau^{-(1/\beta^2)}\} \tag{15}$$

$$= \int_0^\infty d\tau \left[1 + \frac{d}{d\tau} \right] \exp\{-\tau - e^{y/\beta} \tau^{-(1/\beta^2)}\} \equiv g_{(1/\beta)}(y) \tag{16}$$

as the second term in the integrand gives no contribution, being the full derivative of the expression vanishing at the boundaries of the integration region. This transformation

¹⁰ In general such duality holds for the transformation $\beta \rightarrow \beta_c^2/\beta$ but we specialized in this paper to $\beta_c = 1$.

is formal in the sense that the function $g_{1/\beta}(z)$ defined above for $\beta < 1$ has nothing to do with the true generating function in the low temperature phase $\beta > 1$. Rather, it is just obtained by taking the formula valid in the high temperature phase and making the change $\beta \rightarrow 1/\beta$ everywhere. However the duality relation still gives precious information, e.g. it implies that an infinite set of derivatives $(\beta \partial_\beta)^n g_\beta(y) = 0$ for any $n \geq 1$, odd, at the self-dual point $\beta = 1^-$. In particular the exact result

$$\partial_\beta g_\beta(y)|_{\beta=\beta_c^-} = 0, \quad \text{for all } y \tag{17}$$

shows that the ‘flow’ of this function as a function of temperature vanishes at the critical point, quite consistently with a freezing of the whole function (with continuous temperature derivatives). It is in fact quite amazing that precisely this generating function $g_\beta(y) = \overline{\exp(-e^{\beta y} z)}$, with precisely this built-in temperature dependence, is both conjectured to freeze and shown to be self-dual. It is thus tempting to conjecture that freezing and duality are related, i.e. it is $g_\beta(y)$ and no other variation of it (such as e.g. replacing $e^{\beta y}$ by any other function of both y and β) which freezes *because* it is self-dual in the whole high temperature phase. The same type of self-duality relation, as we demonstrate below, extends to the interval case supporting the conjecture.

Unfortunately, the direct methods of resummation which work for the circular case fail for the more complicated problem at hand, the interval $[0, 1]$. For this reason one needs to develop a more general procedure, which is done below.

2.5. From moments to distribution: generalities

Instead here we now define the generic moments $M_\beta(s) = \overline{z^{1-s}}$, $M_\beta(1) = 1$ for any complex s , at fixed inverse temperature β . In particular, the generating function of the cumulants for the free energy $f = -\beta^{-1} \ln z$ is related to $M_\beta(s)$ via

$$\sum_{n=0}^{\infty} \frac{s^n}{n!} \beta^n \overline{f^n} = \ln M_\beta(1 + s). \tag{18}$$

Definition of the probability density $P(z)$ implies the relation

$$\int_{-\infty}^{+\infty} e^{2t} P(e^t) e^{-st} dt = M_\beta(s) \tag{19}$$

which can be inverted as the contour integral

$$e^{-2t} P(e^{-t}) = \frac{1}{2i\pi} \int e^{-st} M_\beta(s) ds, \tag{20}$$

e.g. along a contour parallel to the imaginary axis $s = s_0 + i\omega$, provided the integral is convergent, s_0 being chosen larger than any singularity of the integrand.

Further using the definition (3) the function $g_\beta(y)$ is found to satisfy the identities

$$\beta \int_{-\infty}^{+\infty} e^{\beta y(s-1)} g_\beta(y) dy = M_\beta(s) \Gamma(s - 1) \tag{21}$$

$$g_\beta(y) = \beta^{-1} e^{\beta y} \frac{1}{2i\pi} \int e^{-sy} M_\beta\left(\frac{s}{\beta}\right) \Gamma\left(\frac{s}{\beta} - 1\right) ds. \tag{22}$$

Hence once we know $M_\beta(s)$ we can retrieve all the interesting distributions. Moreover, relation (21) defines after integration by parts the generating function of the cumulants for the probability density defined by $p_\beta(y) = -g'_\beta(y)$:

$$\sum_{n=1}^{\infty} \frac{s^n}{n!} \overline{y^{n^c}} \equiv \ln \int_{-\infty}^{\infty} p_\beta(y) e^{ys} dy = \ln M_\beta \left(1 + \frac{s}{\beta} \right) + \ln \Gamma \left(1 + \frac{s}{\beta} \right). \quad (23)$$

Comparison with (18) yields after recalling the series expansion for $\ln \Gamma(1+s)$ in terms of the Euler constant γ_E and Riemann zeta function $\zeta(n)$ the following model-independent relations:

$$\bar{y} = \bar{f} - \gamma_E T, \quad \overline{y^{n^c}}|_{n \geq 2} = \bar{f}^{n^c} + (-1)^n (n-1)! \zeta(n) T^n. \quad (24)$$

This relation is valid at all temperature and comes only from the definition of $g_\beta(y)$. It is most useful at $\beta = \beta_c = 1$, if we accept the freezing scenario. Given that in that case the lhs freezes at its value at $\beta = 1$ then we easily retrieve all cumulants of the free energy for all $T \leq T_c$ just from the knowledge of $g_{\beta=1}(y)$. Conversely, it is useful to test the freezing hypothesis in numerics, as we will see below.

Let us now discuss how these moment relations reflect duality for the circular case. In the latter model $M_\beta(s) = \Gamma(1 + (s-1)\gamma)$; hence from (23) one finds

$$\sum_{n=1}^{\infty} \frac{s^n}{n!} \overline{y^{n^c}} = \ln \Gamma(1 + s\beta) + \ln \Gamma \left(1 + \frac{s}{\beta} \right) \quad (25)$$

which is manifestly invariant under the formal transformation $\beta \rightarrow 1/\beta$. The latter fact implies, via (23), the self-duality for $p_\beta(y)$, and hence for $g_\beta(y)$. Such an indirect method of proving self-duality for $g_\beta(y)$ has an advantage when direct verification is difficult in view of the cumbersome and/or implicit form for the generating function in the whole high temperature phase. We shall see later on that it does indeed work for the interval case.

3. Analytical continuation at the critical temperature and distribution of minima on the interval

3.1. No edge charges

Let us keep focusing on the critical temperature $\beta = 1$. Defining $M_{\beta=1}(s) \equiv M(s)$, $g_{\beta=1}(y) \equiv g(y)$, we start with the $a = b = 0$ case (no charges at the end of the interval) for the sake of simplicity. For negative integer values $s = 1 - n$ one finds from (10) after exploiting the doubling identity $\Gamma(2z) = 2^{2z-1} \Gamma(z) \Gamma(1/2 + z) / \sqrt{\pi}$ the relation

$$\frac{M(s+1)}{M(s)} = 2^{3+4s} (1+s) \frac{[\Gamma((3/2) + s)]^2}{\pi \Gamma(s) \Gamma(3+s)}. \quad (26)$$

To continue this formula to any s we will use the *Barnes function*, which under some mild conditions is the only solution [21] of

$$G(s+1) = G(s) \Gamma(s) \quad (27)$$

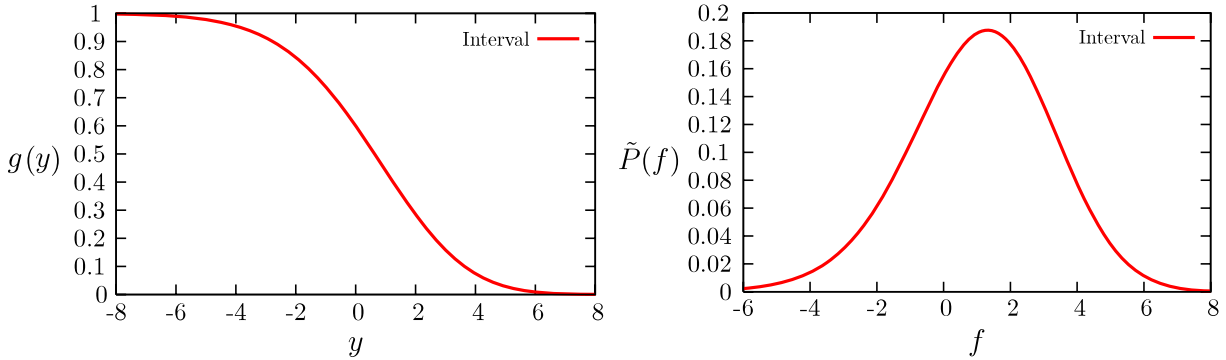


Figure 1. Analytical predictions for the interval $[0, 1]$ with no edge charge: (i), left: plot of $g_{\beta_c}(y)$ which, according to the freezing scenario, is also, up to a shift, the cumulative distribution of the minimum V_{\min} ; (ii), right: the free energy density $\tilde{P}(f)$ at the critical temperature β_c for the interval. Both are obtained by the appropriate inverse Laplace transforms (20) and (22) from the analytical continuation (29) of the moments as indicated in the text.

with $G(1) = 1$. The Barnes function $G(s)$ is meromorphic in the complex plane and has zeros at all negative integers $s = 0, -1, -2, \dots$, [21]. It can be computed as

$$G(z) = (2\pi)^{(z-1)/2} e^{-(1/2)(z-1)(z-2) + \int_0^{z-1} dx x\psi(x)} \quad (28)$$

where $\psi(x) = \Gamma'(x)/\Gamma(x)$, the integral being on any contour not crossing the real negative axis. Using (27) one finds the following analytical continuation for the moments, which is one of the main results of this paper:

$$\overline{z^{1-s}} = M(s) = \frac{2^{2s^2+s-2}}{G(5/2)^2 \pi^{s-1}} \frac{1}{\Gamma(s)\Gamma(s+2)} \left[\frac{G(s+(3/2))}{G(s)} \right]^2 \quad (29)$$

with $G(5/2) = A^{-3/2} \pi^{3/4} e^{1/8} 2^{-23/24}$ where A is Glaisher–Kinkelin constant $A = e^{1/12 - \zeta'(-1)} = 1.28242712$. To guarantee that this is the correct continuation, we have checked: (i) positivity: $M(s)$ given above is finite and positive on the interval $s \in [0, +\infty[$, i.e. all real moments $n = 1 - s < 1$ exist; (ii) convexity: on this interval $\partial_s^2 \ln M(s) > 0$; (iii) convergence of the integrals (20) and (22) for $s_0 > 1$. The latter can be used to compute $g_{\beta=1}(y)$ and $\tilde{P}(f) = e^f / (2\pi i) \int e^{-fs} M(s) ds$, which are plotted in figure 1. Note finally that it reproduces the negative integer moments (11) for $a = b = 0, \gamma = 1$.

The free energy cumulants are to be determined from (23) and (24), and one finds $\langle y \rangle = \frac{7}{2} - 2\gamma_E - \ln(2\pi)$, $\langle y^2 \rangle_c = (4\pi^2/3) - \frac{27}{4}$, and for general $n \geq 3$,

$$\langle y^n \rangle_c = (-)^{n-1} (n-1)! (\zeta(n-1)(2^n - 4) - \zeta(n)(2^{n-3} - k) + 2^{n+1} - 1 - 2^{-n}) \quad (30)$$

with $k = 4$ and the same formula for $\langle f^n \rangle_c$ with $k = 3$. As a comparison for the circle, $M(s) = \Gamma(s)$, hence $\langle y \rangle = 2\langle f \rangle = -2\gamma_E$, and $\langle y^n \rangle_c = 2\langle f^n \rangle_c = 2(-1)^n (n-1)! \zeta(n)$ for $n \geq 2$.

An important property of $g(y)$ at criticality is its decay for $y \rightarrow -\infty$. Deforming the integration contour in (22) one obtains $g(y)$ as a sum of residues over the (multiple) poles

of $M(s)$ at $s = -n$, which generates the expansion in powers of e^y :

$$g(y) = 1 + (y + A')e^y + (A + By + Cy^2 + \frac{1}{6}y^3)e^{2y} \quad (31)$$

$$+ e^y \sum_{n=2}^{\infty} \frac{1}{(2n)!} \partial_s^{2n} e^{-sy} 2^{-(n+1)(2n+3+4s)} \pi^{n+1} \\ \times \frac{\Gamma(n+1+s)^{2n+1} \Gamma(n+3+s) G(s+(3/2))^2 M(n+1+s)}{(s-1)s^2(s+1)^4 \cdots (s+n-1)^{2n-1} G(n+1+s+(3/2))^2} \Big|_{s=-n} \quad (32)$$

with $A' = 2\gamma_E + \ln(2\pi) - 1$ and $C = -0.253846$, $B = 1.25388$, $A = -5.09728$. Let us recall that for the circular model the expression (4) implies

$$g^{(\text{circ})}(y) = 1 + e^y(y - 1 + 2\gamma_E) + e^{2y}(\frac{1}{2}y - \frac{5}{4} + \gamma_E) + \cdots \quad (33)$$

The behavior $g(y) - 1 \sim ye^y$ (see (31) and (33)) is precisely the universal tail found by Carpentier and Le Doussal [6]. It has its origin in the $1/z^2$ forward tail which the probability density of z develops at critical $\beta = 1$, with the first moment $\langle z \rangle$ becoming infinite. On the other side $y \rightarrow +\infty$, one expects much faster decay, for example $g^{(\text{circ})}(y) = \sqrt{\pi} e^{(y/4) - 2e^{y/2}} (1 + \frac{3}{16} e^{-y/2} + \cdots)$.

3.2. Extension to edge charges; the binding transition

Extending these considerations for any a, b , one finds

$$M(s) = 2^{2s^2+s(1+2(a+b))-3-2(a+b)} \pi^{1-s} \\ \times \frac{G(2+a)G(2+b)G(4+a+b)}{\Gamma(2+((a+b)/2))G(2+((a+b)/2))^2 G((5/2)+((a+b)/2))^2} \\ \times \frac{\Gamma(1+((a+b)/2)+s)G(1+((a+b)/2)+s)^2 G((3/2)+((a+b)/2)+s)^2}{G(s)G(1+a+s)G(1+b+s)G(3+a+b+s)} \quad (34)$$

and checks again positivity and convexity for $s \in [0, +\infty[$ (for $a, b > -1$). We give only

$$\overline{y^2}_{a,b}^c = \frac{\pi^2}{6} + \gamma_E + 3\phi(4+a+b) - \phi(2+a) - \phi(2+b) \quad (35)$$

with $\phi(x) = \psi(x) + (x-1)\psi'(x)$, and the case $a = b$ in the limit $a \rightarrow +\infty$ where one then finds

$$\overline{y^2}_{a,a}^c = \ln(8a) + \frac{\pi^2}{6} + \gamma + 1 + O(a^{-1}) \quad \overline{y^3}_{a,a}^c = -\frac{\pi^2}{3} - 2\zeta(3) + O(a^{-1}) + \cdots, \quad (36)$$

i.e. all cumulants have a limit except the second one. This limit is discussed again below.

A remarkable case is $a = b = -1/2$. Then a simplification occurs:

$$M(s) = M_{-1/2,-1/2}(s) = 2^{2s^2-s-1} \pi^{1-s} \frac{\Gamma((1/2)+s)}{s\Gamma(3/2)}. \quad (37)$$

One can trace this simplification to the fact that the structure of the correlation matrix becomes much simpler in that case, as detailed in appendix A. The corresponding

distribution is easily found as (again this is for $\beta = \beta_c = 1$)

$$P(z) = \left(\frac{\pi}{8}\right)^{3/2} \frac{1}{\Gamma(3/2)z^2} \int_0^z \frac{dz_1}{z_1^{3/2}} \int_{-\infty}^{+\infty} \frac{dt}{\sqrt{2\pi}} e^{-(t^2/2) - 3\sqrt{\ln 2}t - (\pi/8)(1/z_1)e^{-2\sqrt{\ln 2}t}} \quad (38)$$

which reproduces the above moments, and behaves as $P(z) \sim \pi/z^2$ at large z . This yields, after some manipulations,

$$g(y) = \frac{\pi}{4} \int_{-\infty}^{+\infty} \frac{dt}{\sqrt{2\pi}} e^{-(t^2/2) - 2\sqrt{\ln 2}t} \int_{e^y}^{\infty} \left(1 - \frac{e^y}{u}\right) e^{-\sqrt{\pi u/2}e^{-\sqrt{\ln 2}t}} du \quad (39)$$

and one finds $\overline{y^2}^c = 4 \ln 2 - 3 + 2\pi^2/3 = 6.35232$ and $\overline{y} = 1 - 2\gamma_E - \ln(\pi/2) = -0.606014$; hence $\overline{f^2}^c = 4 \ln 2 - 3 + \pi^2/2$.

Let us now discuss briefly the case $a, b < -1$; for simplicity we focus on $b = a$. In that case, the model (5) requires, at least naively, a short scale cutoff to avoid the divergence near the edges. However, from e.g. the discussion of appendix D in [6] we know that there should be a competition between the random potential in the bulk and the binding effect by the edge: in the presence of disorder it may be more favorable for the particle to explore the bulk and to remain unbound from the edge. It is quite nice that our analytical continuation captures that effect. As mentioned in section 2.3, from the negative moments one can guess that the complete domain over which the high temperature phase extends is

$$a \geq -1 - \gamma \quad \text{and} \quad \gamma \leq 1 \quad (40)$$

with $\gamma = \beta^2$ (here $\beta_c = 1$), where equality in the first condition corresponds to the binding transition, to the edge, while that in the second corresponds to the freezing transition. This implies in particular that for $\gamma = 1$, the case studied above, the binding transition occurs at $a = -2$, and that for any larger value of a the system should be at bulk critical freezing, with however some continuous dependence in a . We can indeed check that the result (34) for $M(s)$ leads to a well defined probability $P(z)$ for any $a > -2$. For instance one sees that the formula (35) yields a finite $\overline{y^2}^c$ for any $a > -2$, which however diverges as $a \rightarrow -2^+$. The domain of definition becomes $s > -1 - a$ for $-1 > a > -2$, as the resulting $P(z)$ acquires now a broader tail $\sim 1/z^{3+a}$ at large z , while it was $\sim 1/z^2$ for $a > -1$. As $a \rightarrow -2$ the tail becomes non-normalizable as $\sim 1/z$, a signature of the binding transition. The case $a = -3/2$ provides a good illustration as (34) again simplifies to

$$M(s) = M_{-3/2, -3/2}(s) = 2^{2s^2 - 5s + 3} \pi^{1/2 - s} \Gamma(s - \frac{1}{2}) \quad (41)$$

which implies that the random variable z can be written as $z = z_1 e^{-f_2}$ where $z_1 > 0$ and f_2 are two independent random variables, f_2 being Gaussian distributed with $\overline{f_2} = -\ln(2\pi)$ and $\overline{f_2^2}^c = 4 \ln 2$, and z_1 with distribution $P_1(z_1) = z_1^{-3/2} e^{-1/z_1} / \sqrt{\pi}$, leading to the explicit form

$$P(z) = \frac{1}{z^{3/2} \pi \sqrt{8 \ln 2}} \int_{-\infty}^{\infty} dt \exp\left(-\frac{3}{2}t - \frac{1}{z}e^{-t} - \frac{(t + \ln(2\pi))^2}{8 \ln 2}\right) \quad (42)$$

which does exhibit the $\sim 1/z^{3/2}$ tail at large z . We leave further studies of the global phase diagram for arbitrary a, b to the future.

4. The high temperature phase for the $[0, 1]$ interval with no end charges

Let us consider the segment $[0, 1]$ at any $\beta \leq \beta_c = 1$, i.e. $\gamma = \beta^2 < 1$. The moments must satisfy (using again the doubling identity)

$$\frac{M_\beta(s+1)}{M_\beta(s)} = \frac{2^{2+\gamma+4s\gamma}}{\pi} \frac{\Gamma((3/2) + s\gamma)\Gamma(1 + (\gamma/2) + s\gamma)\Gamma((3/2) + (\gamma/2) + s\gamma)}{\Gamma(1 - \gamma + s\gamma)\Gamma(2 + \gamma + s\gamma)\Gamma(1 + s\gamma)}. \quad (43)$$

We need to find a way of continuing the moments to the complex plane. To this end we define the function $G_\beta(x)$ for $\Re(x) > 0$ by [23]

$$\begin{aligned} \ln G_\beta(x) = & \frac{x - Q/2}{2} \ln(2\pi) + \int_0^\infty \frac{dt}{t} \left(\frac{e^{-(Q/2)t} - e^{-xt}}{(1 - e^{-\beta t})(1 - e^{-t/\beta})} \right. \\ & \left. + \frac{e^{-t}}{2}(Q/2 - x)^2 + \frac{Q/2 - x}{t} \right) \end{aligned} \quad (44)$$

where $Q = \beta + 1/\beta$. This function is self-dual:

$$G_\beta(x) = G_{1/\beta}(x) \quad (45)$$

and satisfies the property that we need (see e.g. [23] and appendix B),

$$G_\beta(x + \beta) = \beta^{1/2 - \beta x} (2\pi)^{((\beta-1)/2)} \Gamma(\beta x) G_\beta(x). \quad (46)$$

One can check that $G_\beta(x)$ for $\beta = \beta_c = 1$ coincides with the Barnes function $G(x)$ defined in section 3.1, e.g. setting $\beta = 1$ in (46) one sees that $G_1(x+1) = \Gamma(x)G_1(x)$, and, using $Q = 2$ we have $G_1(1) = 1$. Like the standard Barnes function the new function $G_\beta(x)$ has no poles and only zeros, and these are located at $x = -n\beta - m/\beta$, $n, m = 0, 1, \dots$. It provides us with a natural generalization which can be used to perform the required analytical continuation for any temperature.

Using the above properties we find that

$$\begin{aligned} M_\beta(s) = & A_\beta 2^{(s-1)(2+\beta^2(2s+1))} \pi^{1-s} \\ & \times \frac{\Gamma(1 + \beta^2(s-1))G_\beta(\frac{\beta}{2} + \frac{1}{\beta} + \beta s)G_\beta(\frac{3}{2\beta} + \beta s)G_\beta(\frac{\beta}{2} + \frac{3}{2\beta} + \beta s)}{G_\beta(\beta + \frac{2}{\beta} + \beta s)G_\beta(\frac{1}{\beta} + \beta s)^2} \end{aligned} \quad (47)$$

with

$$A_\beta = \frac{G_\beta((1/\beta) + \beta)^2 G(2\beta + (2/\beta))}{G_\beta((3\beta/2) + (1/\beta))G_\beta((3/2\beta) + \beta)G_\beta((3\beta/2) + (3/2\beta))} \quad (48)$$

reproduces correctly the recursion relation (43), and hence provides an analytical continuation for the moments valid for $\beta < \beta_c = 1$. We have checked numerically that it does satisfy positivity, convexity and a convergent inverse Laplace transform from which one can compute $P(z)$ and $g_\beta(y)$ using (20) and (22). We will not study these in detail here, but give just a few properties.

Let us first check the duality. One easily sees that if one defines

$$M_\beta(s) = 2^{1-s} \tilde{M}_\beta(s), \quad (49)$$

then $\ln \tilde{M}_\beta(1 + (s/\beta)) + \ln \Gamma(1 + (s/\beta))$ is fully invariant under $\beta \rightarrow 1/\beta$. From (23) it implies that all \overline{y}^n with $n \geq 2$ are invariant by duality, only the average \overline{y} is not. This is

not a problem since this average is not expected to be universal, and is easily remedied by defining $\tilde{z} = z/2$ (which could have been done from the start) and $\tilde{g}_\beta(y) = \overline{\exp(-e^{\beta y} z/2)}$. Hence we conclude that up to such a trivial shift the probability $\tilde{p}_\beta(y) = -\tilde{g}'_\beta(y)$ is self-dual, i.e. $\tilde{p}_{1/\beta}(y) = \tilde{p}_\beta(y)$. From the discussion in the previous section we conjecture that it is this function which freezes at $\beta = \beta_c = 1$.

From the result (47) we can extract the cumulants of the free energy using (18). We only discuss here the lowest non-trivial cumulant, given by

$$\overline{f^{2^c}} = \overline{y^{2^c}} - \frac{\pi^2}{6} T^2 = \frac{1}{\beta^2} \partial_s^2 \ln M_\beta(1+s)|_{s=0} \tag{50}$$

$$\begin{aligned} &= 4 \ln 2 + h_\beta \left(\frac{3\beta}{2} + \frac{1}{\beta} \right) + h_\beta \left(\beta + \frac{3}{2\beta} \right) + h_\beta \left(\frac{3\beta}{2} + \frac{3}{2\beta} \right) \\ &\quad - 2h_\beta \left(\beta + \frac{1}{\beta} \right) - h_\beta \left(2\beta + \frac{2}{\beta} \right) + \frac{\beta^2 \pi^2}{6} \end{aligned} \tag{51}$$

where we have defined the self-dual function (see appendix B):

$$h_\beta(x) = h_{1/\beta}(x) = \partial_x^2 \ln G_\beta(x) = \ln x + \int_0^\infty \frac{dt}{t} e^{-xt} \left(1 - \frac{t^2}{(1 - e^{-\beta t})(1 - e^{-t/\beta})} \right) \tag{52}$$

and we have used $\psi'(1) = \pi^2/6$. The resulting curve $\overline{f^{2^c}}$ as a function of β is plotted in figure 11. One finds that it increases from $\overline{f^{2^c}}(\beta \rightarrow 0) = 3$ to $\overline{f^{2^c}}(\beta = 1) = 7\pi^2/6 - 27/4 = 4.76454$. More discussion is given later and in appendix C, together with high temperature expansions.

5. The Gaussian weight model

We now briefly discuss a case where the above considerations fail, and present below some hints as to why this may happen.

We consider now the continuum partition function for the log-correlated field on the full real axis but with a Gaussian weight:

$$Z = \epsilon^{\beta^2} \frac{1}{\sqrt{2\pi}} \int_{-\infty}^\infty dx e^{-x^2/2} e^{-\beta V(x)}.$$

This problem is appealing as it leads to Mehta integrals and moments $z_n^{(G)} = \overline{z^n} = Z^n \Gamma(1 - \beta^2)^n = \prod_{j=1}^{j=n} \Gamma[1 - j\beta^2]$, i.e. simpler expressions than for the interval case considered above.

At criticality $\beta = 1$ this implies $M^{(G)}(s+1)/M^{(G)}(s) = 1/\Gamma(s)$ for $s = -n$, which naturally suggests $M^{(G)}(s) = 1/G(s)$. This is positive for $s > 0$ but, surprisingly, convexity fails for $s > s_c = 1.92586\dots$ Hence this is not an acceptable analytic continuation.

To get another handle on the problem one notes that this model can be obtained from the large a limit of the interval problem $[0, 1]_{aa}$. Writing $x = 1/2 + y$ and performing the change of variable in (7) one finds

$$\lim_{a \rightarrow +\infty} (2\pi)^{-n/2} 2^{2an} (8a)^{(n/2) - ((n(n-1))/2)\gamma} z_n(a, a, \gamma) = z_n^{(G)}(\gamma). \tag{53}$$

J. Stat. Mech. (2009) P10005

Not surprisingly one finds that the pointwise limit

$$M^{(G)}(s) = \lim_{a \rightarrow +\infty} (2\pi)^{-(1-s)/2} 2^{2a(1-s)} (8a)^{(1/2)(1-s^2)} M_{a,a}(s) \tag{54}$$

yields $1/G(s)$ as expected. From this we also get that for large a ,

$$\partial_s^2 \ln M^{(G)}(s) = -\ln(8a) + \partial_s^2 \ln M_{a,a}(s). \tag{55}$$

While the second term is nicely positive for all $s > 0$, the additional factor $-\ln(8a)$ makes the total sum negative for $s > s_c$, violating convexity. In other words while $M_{a,a}(s)$ corresponds to a well defined distribution of probability, corresponding to the problem on the interval with edge charges, $M_G(s)$ corresponds then to this probability ‘convoluted with a Gaussian of negative variance’ and fails to be a probability. Note that such a shift in the second cumulant $\overline{y^2}$ is indeed needed to obtain a finite final result in (36). All higher cumulants $\overline{y^{n^c}}|_{aa}$ with $n \geq 3$ have a nice finite limit as $a \rightarrow \infty$, and can be extracted from the generating function

$$\sum_{n=0}^{\infty} \frac{s^n}{n!} \overline{y^{1+n^c}} = \frac{1}{s} - (s-1)\psi(s) + s - \frac{1}{2} \ln(2\pi) - \frac{1}{2}$$

obtained from $1/G(s)$. Hence the main problem seems to lie in the second cumulant, and one may speculate that it is related to an inadequate treatment of zero-mode fluctuations. Another (possibly related) observation is that for $a \gg 1$ the whole contribution to the $[0, 1]_{aa}$ integral comes from a very small vicinity (of the width of $L_a \sim 1/\sqrt{a}$) of the midpoint $x = 1/2$ of the integration domain. One expects a competition between L_a and the regularization scale for the logarithm, so it may be that the result depends on the order of limits $\epsilon \rightarrow 0$ and $a \rightarrow \infty$. We leave further study of this problem to the future and now turn to numerical studies.

6. Numerical study

6.1. The circular ensemble

We now turn to the numerical checks for the random variables V_i on $i = 1, \dots, M$ grid points and their associated REM of partition function $Z_M = \sum_{i=1}^M e^{-\beta V_i}$. We start with the circular-log ensemble and study the $M \times M$ cyclic correlation matrix (choosing here $W = 0$):

$$C_{ij} = -2 \ln \left(2 \left| \sin \frac{\pi(i-j)}{M} \right| \right) \quad i \neq j, \quad C_{ii} = 2 \ln M + W \tag{56}$$

whose eigenvalues $\lambda_k = 2 \ln M - 2 \sum_{n=1}^{M-1} \cos\{(2\pi/M)nk\} \ln\{2 \sin(\pi/M)n\}$ are all positive, with the uniform mode $\lambda_0 = 0$ for any M . Let us recall that the relation to the continuum model defined above was established in [13] where it was shown that at large M one has $\overline{Z_M^n} = z_n \overline{Z_e^n}$ for $\beta^2 n < 1$ and $\overline{Z_M^n} \sim M^{1+n^2\beta^2}$ for $\beta^2 n > 1$ (the positive moments which formally diverge in the continuum).

The random variables V_i are generated (for M even) as

$$V_l = \sqrt{\frac{2}{M}} \sum_{k=1}^{M/2} \sqrt{\lambda_k} \left[x_k \cos \left\{ \frac{2\pi}{M} kl \right\} + y_k \sin \left\{ \frac{2\pi}{M} kl \right\} \right]$$

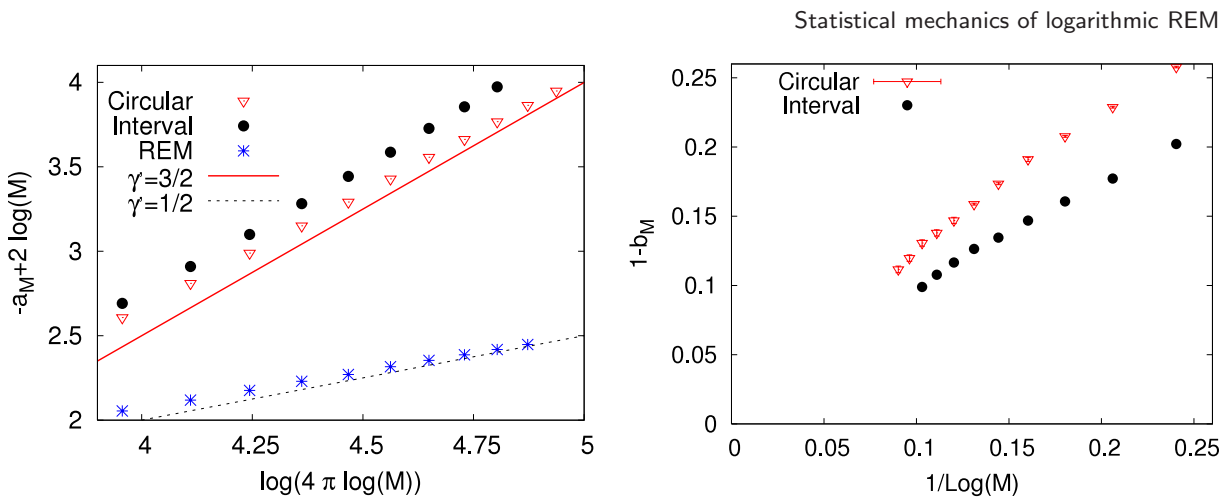


Figure 2. Left: finite size scaling of a_M for variables with logarithmic correlations, circular ensemble equation (56), and interval equation (60), from $M = 2^8$ to 2^{19} . The predicted slope is $\tilde{\gamma} = 3/2$; numerically we find $\tilde{\gamma} = 1.4 \pm 0.1$. This is compared with independent random variables, the standard uncorrelated REM, where the prediction is $\tilde{\gamma} = 1/2$ as observed. Right: finite size effect for b_M for variables with the same correlations. The data are consistent with a convergence as $1/\log M$ and extrapolate to $b_M = 1 \pm 0.02$, consistently with the predicted value $b_M = 1$ in each case (which means an unrescaled variance $\overline{V_{\min}^2}^c$ in agreement with the prediction given in the text, in each case).

where the x_k and y_k are two uncorrelated sets of i.i.d. real unit centered Gaussian variables. This is done using a fast Fourier transform (FFT).

From the distribution of the minimum V_{\min} in systems of up to $M = 2^{19}$ we have computed the coefficients a_M , b_M and the distribution of the variable y in (1) by fixing \bar{y} and the variance $\overline{y^2}^c$ to their value for the distribution (4). The asymptotics of the coefficients a_M and b_M in (1) are shown in figure 2. They exhibit a reasonable agreement with the conjecture (2) with $A = 1$ but one clearly sees that convergence is slow. Convergence to $b_M = 1$ would mean that the prediction $\overline{V_{\min}^2} = \pi^2/3$ is correct. The cumulative distribution $Q_M(y)$ of the rescaled minimum, i.e. the variable y , is shown in figure 3 where the cumulative distribution (4) has been subtracted. One sees that although the difference is small, its convergence, if any, to zero is extremely slow (empirically, $\sim 1/\sqrt{\ln M}$ seems to roughly account for the data, but we do not wish to make any strong claim here).

Then we computed the distribution of the free energy at various temperatures. In figure 4 we have first normalized the free energy distribution to the same average and variance as the unit cumulative Gumbel distribution, i.e. $\exp(-e^x)$, then plotted the difference between the resulting cumulative distribution $Q_{\text{resc}}(f)$ and the Gumbel expression. This shows that the convergence is very fast at $\beta = 1/2$ but rather slow already at $\beta = 1$, where we have little doubt of the result. This is consistent with the fact that the convergence for the minimum is so slow.

To test the freezing scenario we also compute numerically $g_\beta(y)$ for various temperatures. First in figure 5 we test the convergence of the numerically determined $g_{\beta=1}(y, M)$ to the analytical prediction $g_{\beta_c}(y)$ in (4) as a function of M . Then in

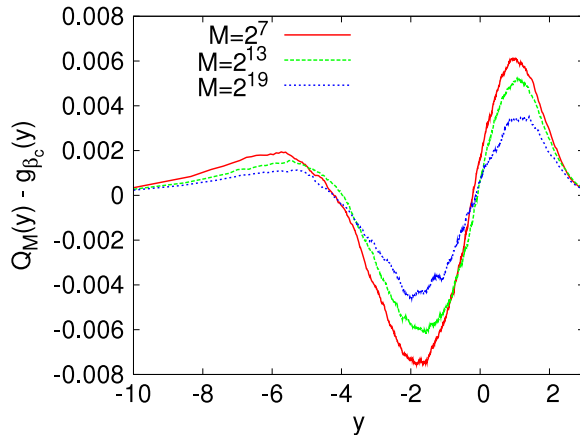


Figure 3. Circular case: cumulative distribution of the rescaled minimum $Q_M(y)$ minus the prediction (4) based on the freezing scenario $g_{\beta_c}(y)$. The number of samples is 10^7 . The difference is small compared on the scale of unity. Although it is slow, the convergence is apparent.

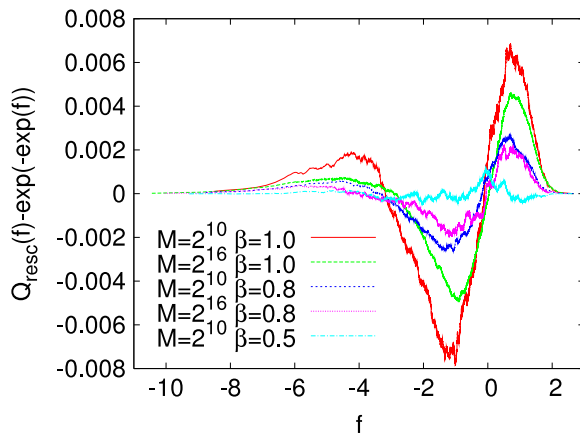


Figure 4. Circular case: distribution of the free energy in the high temperature phase, for various temperatures.

figure 6 we test whether $g_\beta(y, M) - g_{\beta_c}(y, M)$ at fixed $\beta > \beta_c$ decreases to zero as M becomes large, which is the freezing conjecture. In practice we first compute the free energies f_i , compute their mean \bar{f} and variance σ , define rescaled energies $f'_i = (f - \bar{f} + \gamma_E T - 2\gamma_E) \sqrt{(\pi^2/3)(1 - T^2/2)}/\sqrt{\sigma}$ and define $g_\beta(y, M)$ as the mean of $e^{-e^{\beta(y-f'_i)}}$ which, by construction and by virtue of (24), has then the same average, $-2\gamma_E$, and variance, $\pi^2/3$, as $g_{\beta_c}(y)$ in (4). Comparing figures 3 and 5 we see that a good fraction of the difference in figure 3 is already due to finite size corrections at β_c (which have nothing to do with the testing the freezing scenario).

6.2. Universality of the circular ensemble: cyclic matrices, and s GFF inside a disk with a Dirichlet boundary condition

It is important to discuss now the universality of this result, as it is a rather subtle point. The general issue of universality for logarithmic REMs can be formulated as follows.

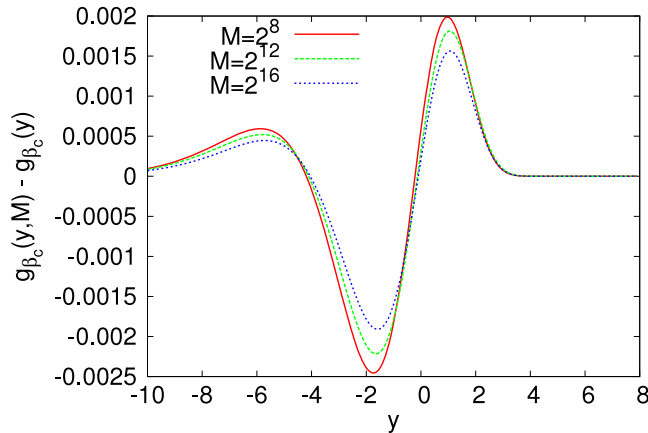


Figure 5. Circular case: convergence of $g_\beta(y, M)$ at $\beta = \beta_c$. We see that the scale is smaller than in figure 2 but that convergence is very slow.

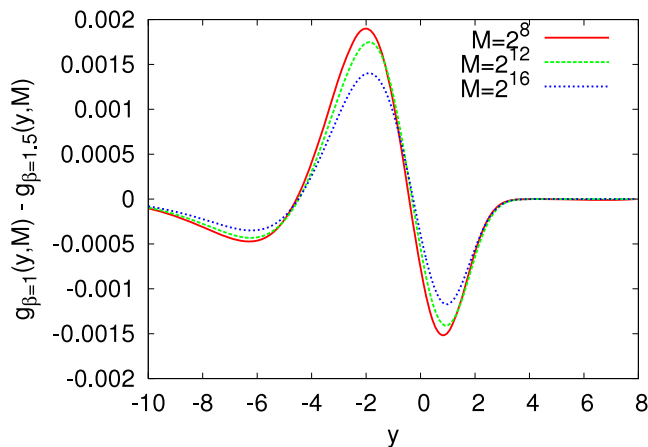


Figure 6. Circular case: direct test of the freezing scenario: convergence of $g_\beta(y, M) - g_{\beta_c}(y, M)$ (both are numerically measured and rescaled as explained in the text). We see that the scale is smaller by a factor around 2–4 than in figure 3, but that convergence is very slow.

Consider sequences of M -dependent correlation matrices $C_{ij}^{(M)}$. What are the possible universality classes for the associated REM in the limit $M \rightarrow +\infty$, what are their basins of attraction and conditions for convergence? One may ask questions for two cases: (i) for extremal universality classes, i.e. correlation matrices which have asymptotically the same distribution of the minimum V_{\min} (up to a shift by an M -dependent constant); (ii) for more restrictive universality classes valid for any β , i.e. correlation matrices which have asymptotically the same distribution of free energy, and generating function $g_\beta(y)$ (up to a shift by an M -dependent constant) for any β . It is reasonable to expect each latter universality class (ii) to correspond to a continuum model. Obviously, two sequences $C_{ij}^{(M)}$ which belong to the same class (ii) also have the same distribution of extrema. But there are counterexamples to the reverse (see below). Classifying these classes being a formidable problem, here we only make a few remarks about the universality class of the circular ensemble. The class corresponding to the interval is discussed below.

Let us start from (56) and discuss various generalizations in the subset of cyclic (called also periodic or circulant) matrices, i.e. which can be written as

$$C_{ij} = \frac{1}{M} \sum_{k=0}^{M-1} \lambda_k e^{2i\pi(i-j)(k/M)}, \quad (57)$$

with (M -dependent) real eigenvalues λ_k . The eigenvalue λ_0 corresponds to the uniform mode (often called the zero mode in the GFF context). Logarithmic correlations mean that we assume that $\lambda_k \sim 1/k$ in some broad range of k at large M , as specified below.

Starting from (56) let us first make the observation that adding a fixed $W > 0$ of $O(1)$ on the diagonal of C_{ij} shifts all eigenvalues by a constant $O(1)$ and does not change the universality class, in both sense (i) and sense (ii), at large M . On the other hand, a shift

$$C_{ij} \rightarrow C_{ij} + \sigma \quad (58)$$

for all (i, j) shifts only the uniform mode $\lambda_0 \rightarrow \lambda_0 + \sigma$. It is equivalent to adding a global random Gaussian shift v to all V_i , i.e. $V_i \rightarrow V_i + v$ where $\sigma = \overline{v^2}$. It thus results in the convolution of the distribution of V_{\min} (and of the free energy) with a Gaussian of variance σ . One such example, discussed again below, is considering the distribution of the GFF (using the full plane Green function) on a circle of radius $R < 1$ (and cutoff $R\epsilon$, i.e. performing a global contraction): it imposes the shift $C_{ij} \rightarrow C_{ij} - 2 \ln R$ in all cases in (56). Hence we keep in mind that there is really *a family of distributions differing by their second cumulant*, and will enforce in our numerics the condition $\lambda_0 = 0$ which we believe selects the distribution (4).

6.2.1. A GFF along an arbitrary circle. One possible generalization of the circular model (56) along these lines is the GFF inside a disk of radius L with $V = 0$ on the boundary as studied by e.g. Duplantier and Sheffield [2]. Using the Dirichlet Green function $G_L(z, z') = -\ln(L|z - z'|)/(|L^2 - z\bar{z}'|)$, the correlation matrix for the discrete model on a circle of radius R inside the disk is then, for $i \neq j$ and writing $\rho = R/L$,

$$C_{ij} = -2 \ln \frac{2\rho |\sin((\theta_i - \theta_j)/2)|}{\sqrt{1 + \rho^4 - 2\rho^2 \cos(\theta_i - \theta_j)}}, \quad C_{ii} = 2 \ln L + 2 \ln(1 - \rho^2) - 2 \ln \epsilon. \quad (59)$$

In the small $\rho = R/L$ limit, equivalently for fixed R and large L one finds $C_{ij} \approx -2 \ln \rho - 2 \ln(2 |\sin((\theta_i - \theta_j)/2)|)$ and $C_{ii} \approx 2 \ln L - 2 \ln \epsilon$. Choosing¹¹ $\epsilon = R/M$ one sees that one does indeed recover the FB model (56) (with $W = 0$) *up to a shift $\sigma = 2 \ln(L/R)$ in the zero mode λ_0* of the matrix, i.e. all eigenvalues of the correlation matrix are the same as those of FB except the uniform mode. This gives us the precise meaning of the universality of the results of FB [13]: it holds for small $\rho = R/L$ for the Dirichlet GFF on the disk and up to a (trivial) convolution with a Gaussian of width $2 \ln(L/R)$. The next question is whether the universality extends to other circular contours on the disk with R/L not necessarily small. The answer is no, as can be argued from examination of the eigenvalues, diagonalizing (59) for arbitrary ρ . As shown in figure 7, at large M the

¹¹ Equivalently one can choose $\epsilon = 1/M$ and $W = -2 \ln R$ which, as we know, does not change the distribution of the maximum.

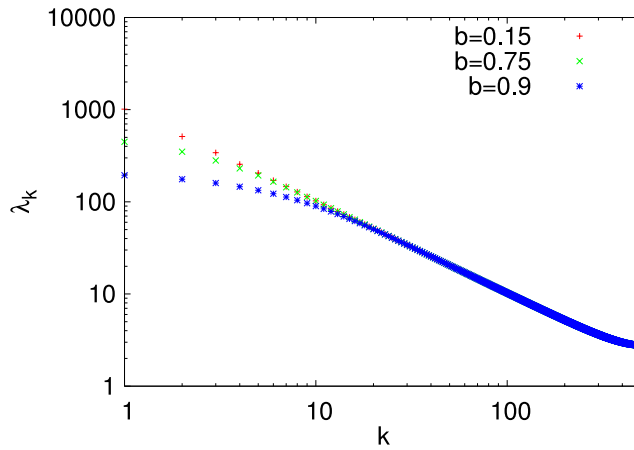


Figure 7. Eigenvalues of the correlation matrix corresponding to the GFF along a circle in a disk domain with zero boundary condition (Dirichlet).

eigenvalues are essentially the same as the ones for FB, i.e. small ρ , apart from the few largest ones—whose number does not change and remains finite as M becomes large. We expect however that since these are the *largest* eigenvalues, despite being few, they will change the distribution of the maximum which hence will depend continuously on the ratio R/L (with a discussion similar to the above concerning the zero mode and convolution with a Gaussian).

6.2.2. Other periodic models. On the other hand a much stronger universality property appears to hold when only the *smallest* eigenvalues are changed. Hence we now test whether the results obtained for the circular case remain valid for all periodic cases (57) with the same behavior of $\lambda_k \sim 1/k$. Again it is important that λ_0 be fixed to zero. If $\lambda_0 > 0$ this amounts to convoluting the distribution of the minimum with a Gaussian of variance λ_0 . For the model to be logarithmic and strong universality to hold we require that $\lambda_k \rightarrow 1/k$ as $M \rightarrow \infty$ for $0 < k \ll M$. We have tested this conjecture for two models.

Model 1: The Sharp model (SM) $\lambda_k = M/k$ for $k = 1, \dots, M/2$ and $\lambda_k = M/(M - k)$ for $k = M/2, \dots, M - 1$.

Model 2: The long range model (LRM) which is some discretization of the Joanny–de Gennes elasticity of the contact line [24], $\lambda_k = 2\pi/\sqrt{2(1 - \cos(2\pi k/M))}$.

The eigenvalues of these models are compared to that of the circular case in figure 8 and one can see that they differ only for k near $M/2$. As can be seen in figure 9, the convergence of these models to the circular case at fixed M is much faster than their (common) convergence to the analytical prediction. We take this as a signature of the strong universality with respect to variations of the correlation matrix which change only the smallest eigenvalues, within the cyclic class. We check in the appendix C that the first terms in the expansion of $\overline{f^2}^c$ are the same for all these models which supports the assertion that the universality holds at any β , i.e. both in sense (i) and in sense (ii) defined above.

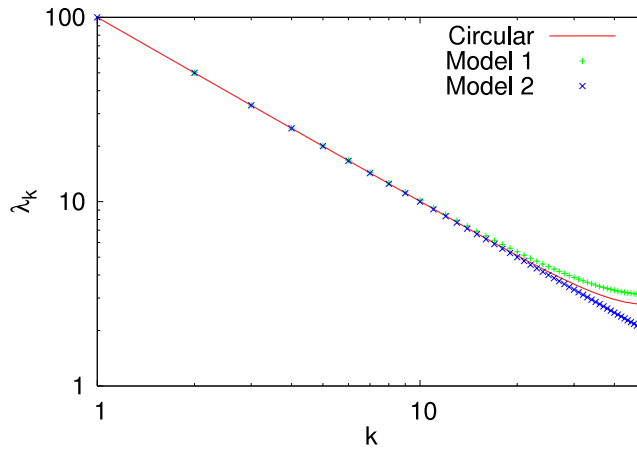


Figure 8. Eigenvalues of the correlation matrix corresponding to the periodic models defined in the text.

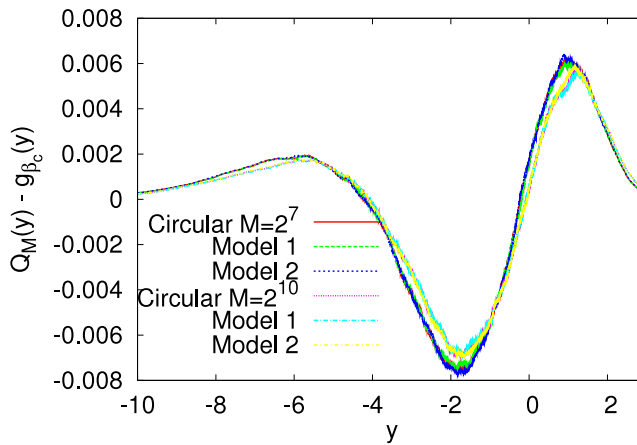


Figure 9. Universality in the case of periodic (circulant) correlation matrices: cumulative distribution of the minimum, with subtraction as in figure 3: convergence to a common curve is faster than to the global analytic prediction.

6.3. The interval

We now discuss the $[0, 1]$ ensemble. We take for the correlation matrix the Toeplitz form $C_{ij} = C(i - j)$, $i, j = 1, \dots, M$:

$$C_{ii} = 4 \sum_1^{M-1} (-1)^k \log \frac{k}{M} + W \quad C_{i \neq j} = -2 \log \frac{|i - j|}{M} \quad (60)$$

with $W = 0$. This matrix is not diagonal in Fourier space and we cannot use the FFT method. In practice we find the eigenvalues λ_k and the normalized eigenvectors $\psi_k(i)$ by a direct diagonalization of the matrix C_{ij} . We then generate the correlated random potential as $V_i = \sum_{k=0}^{M-1} \sqrt{\lambda_k} x_k \psi_k(i)$, where the x_k are i.i.d. real unit centered Gaussian variables. Performing this sum together with the direct diagonalization is numerically

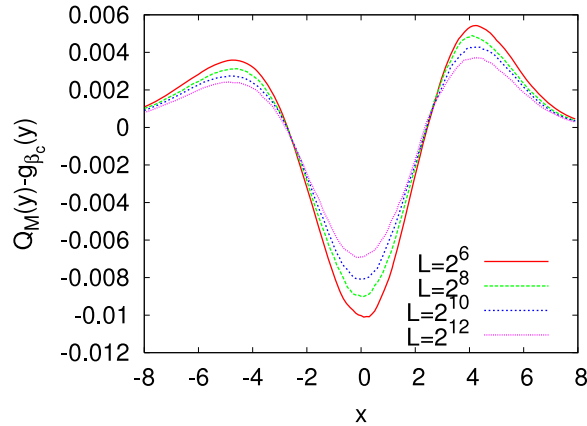


Figure 10. Interval case: cumulative distribution of the rescaled minimum $Q_M(y)$ minus our analytical prediction, $g_{\beta_c}(y)$, shown in figure 1 and based on the freezing scenario. The number of samples is 10^7 . The difference is small compared on the scale of unity. Although it is slow, the convergence is apparent.

expensive and limits the size of the number M of correlated numbers. In order to achieve a good statistics ($\sim 10^7$ samples) we analyze here data only up to $M = 2^{12}$.

To justify our choice for the diagonal element in (60) let us recall a useful property of any Toeplitz matrix: if the function $f(\theta) = C_{11} + 2 \sum_{k=1}^{M-1} C_{1,k+1} \cos(k\theta)$ is positive $\forall \theta \in [0, 2\pi)$, then C is positive definite (for any M). This is seen by noting that for any vector v_k , $k = 0, \dots, M-1$, one has $\sum_{k,\ell=0}^M v_k v_\ell C(k-\ell) = \int_0^{2\pi} (d\theta/2\pi) f(\theta) |v(\theta)|^2$ where $v(\theta) = \sum_{k=0}^{M-1} v_k e^{ik\theta}$ and $C(k) = \int_0^{2\pi} (d\theta/2\pi) f(\theta) e^{ik\theta}$. More importantly it can be shown that the reverse is true for large M [25]. For the choice of equation (60) this function has a global minimum at $\theta = \pi$, for which $f(\theta = \pi) = 0$. As a result the matrix C_{ij} is positive definite and in the large M limit, one finds that the smallest eigenvalue goes rapidly to zero and the eigenvector components alternate as $(-1)^k$. Note that the diagonal element in (60) behaves as $C_{ii} \sim 2 \ln M + O(1)$ at large M —hence as expected, and like for the circular case. Though this is a convenient choice for proving positivity, there are other choices with similar behaviors at large M which would do as well.

We have analyzed the distribution of the minimum V_{\min} and computed the coefficients a_M , b_M and the distribution of the variable y in (1) by fixing $\bar{y} = 7/2 - 2\gamma_E - \ln(2\pi)$ and the variance $\bar{y}^2 = \frac{4}{3}\pi^2 - \frac{27}{4}$ to their value given by the analytical prediction. The convergence to $b_M = 1$, shown in figure 2 (right), is thus a test of our prediction $\overline{V_{\min}^2}^c = \frac{4}{3}\pi^2 - \frac{27}{4}$. The convergence of the coefficients a_M and b_M is quite similar to the circular case. The cumulative distribution $Q_M(y)$ of the rescaled minimum, i.e. the variable y , is shown in figure 10 where the cumulative distribution of figure 1 (our analytical prediction) has been subtracted. Again, the behavior resembles that for the circular case.

The discussion of the universality for the interval class is more delicate since now the lowest eigenvector is no longer generically the uniform mode. However a way to realize it from the GFF can be suggested like in the above discussion. One can consider the interval embedded near the center in a large disk with Dirichlet b.c. In the limit of small ratio ρ of interval size to disk radius the above interval model applies, again up to a convolution with a Gaussian of variance $2 \ln(1/\rho)$.

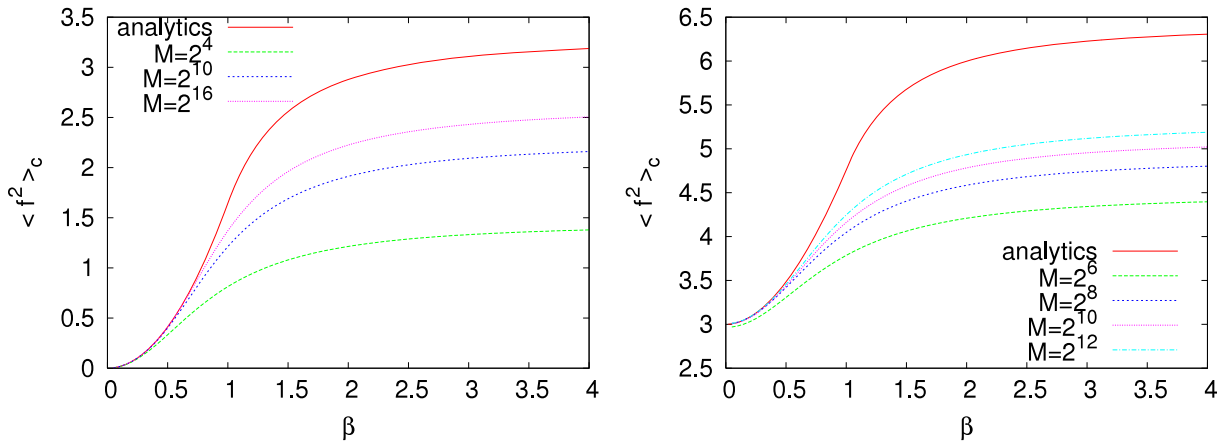


Figure 11. Second cumulant $\overline{f^2}^c$ of the free energy as a function of inverse temperature β for various sizes, as compared to the analytical prediction given in the text. Left: circular ensemble. Right: interval case.

6.4. Temperature dependence of the second cumulant of the free energy

Finally we have also performed some numerical tests of the temperature dependence of our analytical results in the high temperature phase. We have computed numerically, and plotted in figures 11 and 12 as functions of β , the variance of the free energy distribution $\overline{f^2}^c$ as well as $\overline{y^2}^c$ for the circular case (56) and $\overline{f^2}^c$ for the interval case (60). They are compared to the analytical predictions, i.e. (i) for the circular case:

$$\overline{f^2}^c = (\pi^2/6)\beta^2 \quad (\beta < 1) \quad \text{and} \quad \overline{f^2}^c = (\pi^2/6)(2 - T^2) \quad (\beta > 1), \quad (61)$$

which via equation (24) corresponds to $\overline{y^2}^c = (\pi^2/6)(\beta^2 + (1/\beta^2))$ for $\beta < 1$ which freezes into $\overline{y^2}^c = \pi^2/3$ for $\beta > 1$, and (ii) for the interval case formula (50) for $\beta < 1$ and $\overline{f^2}^c(\beta) = \overline{f^2}^c(\beta_c = 1) + (\pi^2/6)(1 - T^2)$ for $\beta > 1$. One can verify the good convergence in the high temperature phase. Questions related to the behavior for small β , and how the numerical convergence could be further improved, are discussed in the appendix C.

6.5. More open questions on universality

Let us now indicate a simple example where universality (i) of distribution of the minimum and (ii) of the free energy at any temperature, discussed above, may differ from each other. Consider the continuum problem on the circle but with an arbitrary smooth and nonsingular weight $0 < \rho_1 < \rho(\theta) < \rho_2 < 1$:

$$Z = \epsilon^{\beta^2} \int_0^{2\pi} d\tilde{\theta} \rho(\tilde{\theta}) e^{-\beta V(e^{i\tilde{\theta}})} = \epsilon^{\beta^2} \int_0^{2\pi} d\theta e^{-\beta V(e^{if(\theta)})} \quad (62)$$

and we consider for instance $\tilde{\theta} = f(\theta) = \theta + a \sin(\theta)$ with $a < 1$ and $\rho(\tilde{\theta}) = 1/f'(\theta)$. From the second form in (5) one sees that the associated REM can be chosen as $Z_M = \sum_i e^{-\beta V_i}$ with correlation matrix $C_{ij} = -2 \ln |2 \sin(\frac{1}{2}f(\theta_i) - \frac{1}{2}f(\theta_j))|$ for $i \neq j$ and $\theta_i = 2\pi i/M$, neither a circulant nor a Toeplitz matrix. As shown in appendix C, at small a , $\overline{f^2}^c = \frac{1}{2}a^2 + O(a^4) + O(\beta^2)$; hence the free energy distribution clearly depends

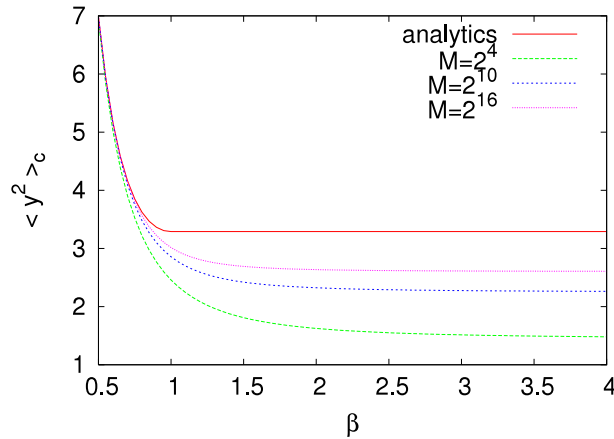


Figure 12. Circular case: second cumulant $\overline{y^2}^c$ as a function of inverse temperature β for various sizes M as compared to the analytic prediction given in the text.

on a . On the other hand, the first form in (62) suggests that it should have the same distribution of the minimum V_{\min} as $\rho(\theta) = 1$. Indeed, $V(\theta) - T \ln \rho(\theta)$ as $T \rightarrow 0$ should have same extremal statistics for a given ϵ regularization (with $T \rightarrow 0$ before $\epsilon \rightarrow 0$) as $V(\theta)$ provided $\rho(\theta)$ is nonsingular. The questions of how the freezing scenario works in such circumstances and what the universality classes are will be left for future studies.

Finally, another challenging question about universality, related to the GFF, is about REMs constructed along curves in the plane different than the circle, or in an interval, i.e. $V_i = V(z_i)$, where the z_i lie along a curve and sample it at large M with a density described in terms of some given arc length $\sqrt{dz d\bar{z}} \rho(z, \bar{z})$. One can use conformal maps to relate various curves to each other, e.g. a circle to a slightly deformed circle, with different weight functions $\rho(z, \bar{z})$. Hence we are back to understanding the type of problem described in the preceding paragraph, and one should expect some universality in the distribution of the minimum.

7. Conclusion

To summarize, we have studied analytically and numerically random energy models based on Gaussian random potentials with logarithmic correlations. We have extended the Fyodorov–Bouchaud (FB) results from the circular ensemble to the interval. We have found the proper analytic continuation from the positive integer moments of the partition function, expressed as Selberg integrals, to arbitrary moments. This analytic continuation of the Selberg integrals, previously an outstanding open problem, is solved here. The solution involves Barnes functions and their generalizations which appear in studies of the Liouville field theory, hence strengthening the already noted link between the two problems. This solution, valid in the high temperature phase, allowed us to obtain the full distribution of the free energy f for $\beta \leq \beta_c$ and up to the critical point. It was generalized, at $\beta = \beta_c$, to the case where additional charges exist at the end of the interval.

The knowledge of the generating function $g_\beta(y) = \overline{\exp(-e^{\beta(y-f)})}$ at $\beta = \beta_c$ allowed us, via the same *freezing scenario* hypothesis as was put forward by FB for the circular ensemble, to obtain the distribution of the minimum of the Gaussian free field (GFF) on an interval, expressed as an integral transform of a Barnes function. The freezing scenario, which asserts that precisely this generating function $g_\beta(y)$ becomes temperature independent in the glass phase for $\beta \geq \beta_c$, was until now based on a traveling wave analysis. While rigorous for the Cayley tree based REM, for which it was introduced, it was only based on a one-loop RG analysis for the type of model at hand [6]. Here we made what we believe should be considered as a step towards better understanding of this freezing scenario: we discovered that, both for the circular ensemble and for its interval counterpart, the analytic expression for $g_\beta(y)$ obeys, in the high temperature phase, duality with respect to the transformation $\beta \rightarrow 1/\beta$. This implies in particular $\partial_\beta g_\beta(y) = 0$, for all y , at $\beta = \beta_c$, in perfect agreement with a continuous freezing scenario. While one may notice that the generating function $g_\beta(y)$ is special, being the partition function of the Liouville *model* (see e.g. the discussion in [6]), further connections to duality in Liouville *field theory* remain to be understood (the high temperature phase being the analog of the weak coupling phase in the Liouville case).

Detailed numerical calculations of the free energy distribution and of the function $g_\beta(y)$ associated with discrete REM versions of the circular and interval models were performed. The freezing scenario is consistent with our results, in both cases, though convergence is found to be very slow. The numerically obtained distribution of the minimum V_{\min} of M random Gaussian variables V_i with logarithmic correlation matrices C_{ij} is found to lie close to the predictions, but with only very slow convergence as a function of M . In the high temperature phase the convergence to the FB result for the circular case and to the present one for the interval is found to be very convincing, and in full agreement with various high temperature expansions also performed here.

The important question of the universality classes for discrete REMs based on logarithmic matrices C_{ij} and for their continuum analogs is discussed. The continuum circular ensemble of FB is found to provide a single universality class for all circulant matrices with appropriate behavior of their spectrum at large M , for which we provide several examples. This strong version of universality holds for any temperature, i.e. identical distribution of free energy for all β , up to a shift. A weaker version of universality, holding only for the distribution of the minimum V_{\min} , is discussed through an example. As far as the connection to the GFF is concerned, we discuss the case where the field is sampled along a circle of radius R inside a disk of radius L with Dirichlet boundary condition. We demonstrate universality, *up to the convolution with a Gaussian*, in the limit of a small ratio R/L , while in general the distributions depend on the aspect ratio R/L .

The present progress opens many more fascinating questions. First one would want to extend these results to other curves in the plane, and even to two-dimensional regions. The simplest extension, i.e. the case of the real axis with Gaussian weight, also studied here, and for which the present methods are found to fail, shows that more remains to be understood before this can be achieved. Unbounded regions seem to pose a problem, and so does the control of the zero mode. The question of classifying the universality classes remains a tantalizing open question. One can expect that the conformal invariance of the 2D GFF will play a crucial role in that classification, as it allows us to map one

curve into another one, with a change in the local length element. The questions of which models obey duality and what is the precise connection to the freezing scenario are also outstanding. Further exploration of the connection to the Liouville model, to the Liouville field theory and to Liouville quantum gravity measures is an important direction for further research. In particular, the distribution of the length of a segment in Liouville quantum gravity seems to directly connect to our results.

Acknowledgments

We are grateful to I Gruzberg and P Wiegmann for useful discussions at various stages of the project. YF acknowledges support by the Leverhulme Research Fellowship project ‘A single particle in random energy landscapes’ and PLD from ANR program 05-BLAN-0099-01.

Appendix A. The special case of $[0, 1]_{-1/2, -1/2}$

Here we study the model defined by the partition sum

$$Z = \int_{-1}^{+1} \frac{dx}{\sqrt{1-x^2}} e^{\beta V(x)} \quad (\text{A.1})$$

$$\overline{V(x)V(x')} = -2 \ln |x - x'| \quad (\text{A.2})$$

which is a special case of the interval $[0, 1]_{ab}$ defined in the text for $a = b = -1/2$. We show that it corresponds to a REM with a correlation matrix which can be diagonalized in the Fourier basis.

Using the change of variable $x = \cos \theta$, and hence $dx = \sin \theta d\theta = \sqrt{1-x^2} d\theta$, we see that Z can also be written as an integral over a half-circle, involving a new Gaussian random potential with a modified correlator:

$$Z = \int_0^\pi d\theta e^{\beta \tilde{V}(\theta)} \quad (\text{A.3})$$

$$\overline{\tilde{V}(\theta)\tilde{V}(\theta')} = -2 \ln |\cos(\theta) - \cos(\theta')| = \sum_{n=1}^{\infty} \frac{4}{n} \cos(n\theta) \cos(n\theta') + 2 \ln 2 \quad (\text{A.4})$$

where we have used the formula

$$\sum_{n=1}^{\infty} \frac{2}{n} \cos(nA) \cos(nB) = -\ln(2|\cos A - \cos B|). \quad (\text{A.5})$$

To define the corresponding REM we now take a grid $\theta = 2\pi i/M$ for *the full circle* and take for correlation matrix

$$C_{ij} = \sum_{n=1}^{\infty} \frac{4}{n} \cos(2n\pi i/M) \cos(2n\pi j/M) + 2 \ln 2 \quad (\text{A.6})$$

for $i \neq j$. The sum is still infinite, but it has the nice property that it can be made finite. Indeed using that

$$\cos(2(k+mM)\pi i/M) \cos(2(k+mM)\pi j/M) = \cos(2k\pi i/M) \cos(2k\pi j/M) \quad (\text{A.7})$$

we can now write

$$C_{ij} = \sum_{n=1}^M \lambda_n \cos(2n\pi i/M) \cos(2n\pi j/M) + 2 \ln 2 \quad (\text{A.8})$$

$$\lambda_n = \frac{1}{n} + \sum_{m=1}^{\infty} \left(\frac{1}{n+mM} - \frac{1}{mM} \right) = \frac{1}{n} - \frac{\gamma + \psi(1 + (n/M))}{M}. \quad (\text{A.9})$$

One can check numerically that all the eigenvalues are positive. Note that we have subtracted an infinite part on the diagonal so now the diagonal element is also well defined:

$$C_{ii} = \sum_{n=1}^M \lambda_n \cos(2n\pi i/M)^2 + 2 \ln 2. \quad (\text{A.10})$$

Hence for this particular interval model $a = b = -1/2$ we can use the Fourier basis to generate the variables on the full circle and take the minimum only for the half-circle (i.e. the $M/2 \times M/2$ submatrix). It remains to be understood how this links to the simplification observed in formula (37) in the text, and whether there are other examples of such cases where a Fourier basis can be used.

Appendix B. Some properties of the generalized Barnes function

Let us first check that the function $G_\beta(x)$ defined by (44) does indeed satisfy the property (46). We start from the formula (see [22] 8.341.3, p. 889)

$$\ln \Gamma(x\beta) = \int_0^\infty \frac{dt}{t} \left[\frac{e^{-\beta xt} - e^{-t}}{1 - e^{-t}} + e^{-t}(\beta x - 1) \right]. \quad (\text{B.1})$$

Now, by straightforward algebra, (44) implies

$$\ln G_\beta(x + \beta) - \ln G_\beta(x) = \frac{\beta}{2} \ln(2\pi) + \int_0^\infty \frac{dt}{t} \left[\frac{e^{-xt}}{(1 - e^{-t/\beta})} + \frac{e^{-t}}{2}(2\beta x - 1) - \frac{\beta}{t} \right]. \quad (\text{B.2})$$

Making now the change $t \rightarrow \beta t$, and subtracting (B.1) gives

$$\phi_\beta(x) \equiv \ln G_\beta(x + \beta) - \ln G_\beta(x) - \ln \Gamma(x\beta) - \frac{\beta}{2} \ln(2\pi) \quad (\text{B.3})$$

$$= \int_0^\infty \frac{dt}{t} \left[\frac{e^{-t}}{1 - e^{-t}} - \frac{e^{-t\beta}}{2} + \beta x (e^{-t\beta} - e^{-t}) + e^{-t} - \frac{1}{t} \right]. \quad (\text{B.4})$$

Now using the identity

$$\int_0^\infty \frac{dt}{t} (e^{-t} - e^{-t\beta}) = \ln \beta \quad (\text{B.5})$$

we see that $(\partial/\partial x)\phi_\beta(x) = -\beta \ln \beta$ which implies

$$\phi_\beta(x) = -\beta x \ln \beta + \phi_\beta(0),$$

with

$$\phi_\beta(0) = \int_0^\infty \frac{dt}{t} \left(\frac{e^{-t}}{1 - e^{-t}} - \frac{e^{-t\beta}}{2} + e^{-t} - \frac{1}{t} \right). \tag{B.6}$$

In turn, it is easy to see this integral converges and $(d/d\beta)\phi_\beta(0) = (1/2\beta)$, and hence $\phi_\beta(0) = \frac{1}{2} \ln \beta + \phi_{\beta=1}(0)$. Combining the above, we see that $\phi_\beta(x) = (\frac{1}{2} - \beta x) \ln \beta + c$, where

$$c = \int_0^\infty \frac{dt}{t} \left(\frac{e^{-t}}{1 - e^{-t}} + \frac{e^{-t}}{2} - \frac{1}{t} \right) \equiv \lim_{z \rightarrow 0} \int_0^\infty \frac{dt e^{-zt}}{t} \left(\frac{1}{e^t - 1} + \frac{1}{2} - \frac{1}{t} \right) + \int_0^\infty \frac{dt e^{-zt} e^{-t} - 1}{t \cdot 2} \tag{B.7}$$

which, using [22] 8.341.1, p. 888, yields

$$c = \lim_{z \rightarrow 0} \left[\ln \Gamma(z) + z - (z - 1/2) \ln z - \frac{1}{2} \ln 2\pi + \int_0^\infty \frac{dt e^{-zt} e^{-t} - 1}{t \cdot 2} \right]. \tag{B.8}$$

The last integral is equal to $\frac{1}{2} \ln(z/(z + 1))$, and after straightforwardly taking the limit we find finally $c = -\frac{1}{2} \ln 2\pi$, in full agreement with (46).

Next we want to obtain the asymptotics. For this it is useful to note that

$$h_\beta(x) := \partial_x^2 \ln G_\beta(x) = \int_0^\infty \frac{dt}{t} \left(e^{-t} - \frac{t^2 e^{-xt}}{(1 - e^{-\beta t})(1 - e^{-t/\beta})} \right). \tag{B.9}$$

Exploiting again the identity (B.5) we can rewrite the above formula in a form more convenient for applications; see equation (52) in the text. For example, by making the change of variables $t = \tau/x$ in (52) we can immediately find the asymptotic behavior for $x \rightarrow \infty$ at fixed β to be given by

$$h_\beta(x) = \ln x - \frac{1}{2x} \left(\beta + \frac{1}{\beta} \right) + \dots$$

as long as $x \gg \max(\beta, \beta^{-1})$. The same asymptotic behavior holds for $h_\beta(z)$ in the complex plane for $\Re z > 0$ and $|z| \rightarrow \infty$.

Note also the useful doubling formula (N.1) for $G_\beta(x)$ which we were not able to trace in the available literature.

Appendix C. High temperature expansions

C.1. High temperature expansion of REM models

It is useful to derive high temperature expansions for a Gaussian REM $Z_M(\beta) = \sum_{i=1}^M e^{-\beta V_i}$ with an arbitrary correlation matrix $\overline{V_i V_j} = C_{ij}$. One uses the expansion

$$Z_M(\beta) = M - \beta \sum_i V_i + \frac{1}{2} \beta^2 \sum_i V_i^2 - \frac{1}{6} \beta^3 \sum_i V_i^3 + O(\beta^4) \tag{C.1}$$

which leads to

$$\begin{aligned} \ln Z_M(\beta) = \ln M - \frac{\beta}{M} \sum_i V_i + \frac{1}{2} \beta^2 \left(\frac{1}{M} \sum_i V_i^2 - \frac{1}{M^2} \sum_{ij} V_i V_j \right) \\ - \frac{1}{6} \beta^3 \left(\frac{1}{M} \sum_i V_i^3 - 3 \frac{1}{M^2} \sum_{ij} V_i V_j^2 + 2 \frac{1}{M^3} \sum_{ijk} V_i V_j V_k \right) + O(\beta^4). \end{aligned} \quad (\text{C.2})$$

This leads to the average free energy

$$F_M(\beta) = -\frac{1}{\beta} \overline{\ln Z_M(\beta)} = -\frac{1}{\beta} \ln M - \frac{1}{2} \beta \left(\frac{1}{M} \sum_i C_{ii} - \frac{1}{M^2} \sum_{ij} C_{ij} \right) + O(\beta^3) \quad (\text{C.3})$$

and the variance

$$\begin{aligned} \overline{f^2}^c = \frac{1}{\beta^2} \overline{\ln^2 Z_M(\beta) - \ln Z_M(\beta)^2} = \frac{1}{M^2} \sum_{ij} C_{ij} + \beta^2 \left(\frac{1}{M^2} \sum_{ij} (C_{ii} C_{ij} + \frac{1}{2} C_{ij}^2) \right. \\ \left. - \frac{1}{M^3} \sum_{ijk} (3C_{ij} C_{ik} + C_{ii} C_{jk}) + \frac{5}{2} \frac{1}{M^4} \sum_{ijkl} C_{ij} C_{kl} \right) + O(\beta^4). \end{aligned} \quad (\text{C.4})$$

This result for $\overline{f^2}^c$ is useful for testing universality in the sense (ii), i.e. at any temperature. Let us examine several cases.

Consider first the periodic case discussed in the text, where C_{ij} is a cyclic (i.e. circulant) matrix, i.e. of the form (57). Then $(1/M^2) \sum_{ij} C_{ij} = \lambda_0/M$. Fixing $\lambda_0 = 0$ as we did here, we find that the expression for the second cumulant of the free energy simplifies and that it vanishes at $\beta = 0$ as

$$\overline{f^2}^c = \frac{\beta^2}{2M^2} \text{Tr} C^2 + O(\beta^4) = \frac{\beta^2}{2M^2} \sum_{k \neq 0} \lambda_k^2 + O(\beta^4). \quad (\text{C.5})$$

It is now easy to check that the discrete circular model (56), the Sharp model (SM) and the long range model (LRM) behave in the limit $M \rightarrow +\infty$ as

$$\overline{f^2}^c = \beta^2 \sum_{k=1}^{\infty} \frac{1}{k^2} + O(\beta^4) = \frac{\pi^2}{6} \beta^2 + O(\beta^4), \quad (\text{C.6})$$

i.e. as the continuum circular model for which one has (61). This is consistent with the conjecture that these models belong to the same universality class at any temperature. Furthermore the coefficient of β^2 can also be obtained, e.g. for the discrete circular ensemble (56), as

$$\lim_{M \rightarrow \infty} \frac{1}{2M^2} \sum_{ij} C_{ij}^2 = \frac{1}{2} \int_0^{2\pi} \frac{d\theta_1}{2\pi} \int_0^{2\pi} \frac{d\theta_2}{2\pi} \left[2 \ln 2 \left| \sin \left(\frac{\theta_1 - \theta_2}{2} \right) \right| \right]^2 = \frac{\pi^2}{6}. \quad (\text{C.7})$$

Note that the diagonal does not contribute to this limit (its contribution is $O(\ln^2 M/M)$) and that will be a general fact.

For the discrete interval model (60) we compute the two first terms in the high temperature expansion. We see that the terms involving C_{ii} cancel out, as they should.

In the limit $M \rightarrow \infty$ we replace remaining sums by integrals and get

$$\overline{f^2}^c = -2I_0 + 2\beta^2 \left[I_1 + 5I_0^2 - 6\tilde{I} \right] + O(\beta^4), \quad (\text{C.8})$$

where we have defined the integrals

$$I_0 = \int_0^1 dx_1 \int_0^1 dx_2 \ln |x_2 - x_1|, \quad I_1 = \int_0^1 dx_1 \int_0^1 dx_2 \ln^2 |x_2 - x_1| \quad (\text{C.9})$$

$$\tilde{I} = \int_0^1 dx_1 \int_0^1 dx_2 \int_0^1 dx_3 \ln |x_2 - x_1| \ln |x_3 - x_1|. \quad (\text{C.10})$$

Calculation of these integrals gives

$$I_0 = -3/2, \quad I_1 = \frac{7}{2}, \quad \tilde{I} = \frac{17}{6} - \frac{\pi^2}{18}$$

which gives the final result

$$\overline{f^2}^c = 3 + \beta^2 \left[\frac{2}{3}\pi^2 - \frac{9}{2} \right] + O(\beta^4). \quad (\text{C.11})$$

As we show below, this coincides with our analytical prediction from the continuum model; see (C.17) below.

As we see in figure 11, for the discrete interval model (60) at finite M , $\overline{f^2}^c(\beta = 0)$ is smaller than 3. In fact, one can add a W_M on the diagonal in (60) so as to tune this value to exactly 3 for any M , without changing the universality class (i.e. W_M goes to zero fast enough). One could try to systematize this idea, e.g. to add to the correlation matrix of the discrete model some other matrix, subdominant in the limit $M \rightarrow \infty$, so as to fit the lowest order coefficients in β^p to their actual values for the continuum model—those are given below for the interval; see formula (C.17). We have checked for the circular case that it can be easily implemented up to $p = 2$. Whether this will allow us to select better discrete models with faster convergence even at lower temperature is left for future studies.

Concerning the class of model (5), we can similarly check that for the associated discrete REM, i.e. $C_{ij} = -2 \ln |2 \sin(\frac{1}{2}f(\theta_i) - \frac{1}{2}f(\theta_j))|$ for $i \neq j$ and $\theta_i = 2\pi i/M$, one has

$$\begin{aligned} \lim_{M \rightarrow \infty} \frac{1}{M^2} \sum_{ij} C_{ij} &= -2 \int_0^{2\pi} \frac{d\theta_1}{2\pi} \int_0^{2\pi} \frac{d\theta_2}{2\pi} \ln \left[2 \left| \sin \left(\frac{f(\theta_1) - f(\theta_2)}{2} \right) \right| \right] \\ &= \frac{1}{2}a^2 + O(a^4) \end{aligned} \quad (\text{C.12})$$

for $f(\theta) = \theta + a \sin(\theta)$; hence at small a , $\overline{f^2}^c = \frac{1}{2}a^2 + O(a^4) + O(\beta^2)$ as announced in the text, and there is no universality valid at all temperature (the universality class in the sense (ii) defined above depends on the function $f(\theta)$).

Finally the same expansion (C.4) holds for any continuum REM of the form $Z = \int dx \rho(x) e^{-\beta V(x)}$ and can be obtained from the above just by making the replacement $(1/M^n) \sum_{i_1, \dots, i_n} \rightarrow (1/(\int dx \rho(x))^n) \int_{x_1, \dots, x_n}$ and replacing C_{i_1, i_2} by its continuum expression $C(x_1, x_2)$.

C.2. High temperature expansion of the analytical result for the interval

Let us derive the high temperature expansion of our analytical result (50)–(52) for the second cumulant of the free energy. Since an independent method also exists for obtaining this expansion, as displayed in the discussion above, this constitutes a check of our solution for the high temperature phase. For this we need to use (52) for $x = \alpha_1\beta + \alpha_2(1/\beta)$, where $\alpha_{1,2}$ are given positive constants. On introducing $\tau = t/\beta$ we have

$$h_\beta \left(\alpha_1 \beta + \frac{\alpha_2}{\beta} \right) = \ln \frac{\alpha_2}{\beta} + \ln \left(1 + \frac{\alpha_1}{\alpha_2} \beta^2 \right) + \int_0^\infty \frac{d\tau}{\tau} e^{-\alpha_2\tau - \alpha_1\beta^2\tau} \times \left(1 - \frac{\tau^2\beta^2}{(1 - e^{-\beta^2\tau})(1 - e^{-\tau})} \right) \tag{C.13}$$

which can be easily used for expanding in powers of β^2 . In particular, the leading term from (50) is a constant given by

$$\overline{f^2}^c = 2 \ln 3 + \ln 2 + \int_0^\infty \frac{d\tau}{\tau} \left(1 - \frac{\tau}{1 - e^{-\tau}} \right) (2e^{-(3/2)\tau} - e^{-\tau} - e^{-2\tau}) \tag{C.14}$$

where the integral can be computed in pieces using the formulae (see 3.311.7 [22])

$$\int_0^\infty d\tau \frac{e^{-\mu\tau} - e^{-\nu\tau}}{1 - e^{-\tau}} = \psi(\nu) - \psi(\mu), \quad \text{and} \quad \int_0^\infty \frac{d\tau}{\tau} (e^{-\mu\tau} - e^{-\nu\tau}) = \ln \frac{\nu}{\mu}. \tag{C.15}$$

Combining the above, we find

$$\overline{f^2}^c(\beta = 0) = 4 \ln 2 - [\psi(1) + \psi(2) - 2\psi(3/2)] = 3, \tag{C.16}$$

in agreement with the result obtained above in (C.9) by a direct method.

This expansion can be carried to higher order. Using Mathematica and some heuristics we find that it can be put in the form

$$\overline{f^2}^c = 3 + \left(\frac{2}{3}\pi^2 - \frac{9}{2} \right) \beta^2 + \sum_{k=2}^\infty (-1)^{k+1} 3k \left(\zeta(k+1) - \left(1 + \frac{B_k}{k} \right) \right) \beta^{2k} \tag{C.17}$$

where the B_k are the Bernoulli numbers ($B_k = 0$ for k odd).

Note added. After submission, we learned of a recent independent study by Ostrovsky [26] who obtained a high temperature expansion of arbitrary moments for the $[0, 1]$ problem with no edge charges, and conjectured a formula for these moments. Exploiting the integral representation (44) for the generalized Barnes function $G_\beta(z)$ together with the following doubling formula:

$$G_\beta(2z) = C_\beta 2^{2z^2 - (1+\beta+(1/\beta))z} \pi^{-z} G_\beta(z) G_\beta \left(z + \frac{1}{2\beta} \right) G_\beta \left(z + \frac{\beta}{2} \right) G_\beta \left(z + \frac{1}{2\beta} + \frac{\beta}{2} \right) \tag{N.1}$$

where C_β is determined from e.g. $z = 1$, we were able to show that his conjecture is equivalent to our formula (47). Note however that no discussion of the critical case, duality and freezing is given in [26]. We have also shown that using Dirichlet boundary conditions at large distance $|x| = L$ for the 2D GFF gives a proper meaning to the problematic Gaussian weight case (at β_c it yields a shift $2 \ln L$ in the second cumulant $\overline{y^2}$, while maintaining all higher cumulants as given in the text).

References

- [1] Di Francesco P, Mathieu P and Senechal D, 1997 *Conformal Field Theory* (Berlin: Springer)
- [2] Duplantier B and Sheffield S, 2009 arXiv:0901.0277
Duplantier B and Sheffield S, 2008 arXiv:0808.1560
- [3] Aarts D G A L, Schmidt M and Lekkerkerker H N W, 2004 *Science* **304** 847
- [4] Chamon C, Mudry C and Wen X-G, 1996 *Phys. Rev. Lett.* **77** 4194
Castillo H E, Chamon C C, Fradkin E, Goldbart P M and Mudry C, 1997 *Phys. Rev. B* **56** 10668
- [5] Fyodorov Y V, 2009 *J. Stat. Mech.* P07022 [arXiv:0903.2502]
- [6] Carpentier D and Le Doussal P, 2001 *Phys. Rev. E* **63** 026110
- [7] Abdalla E and Tabar M R R, 1998 *Phys. Lett. B* **440** 339
- [8] Astala K, Jones P, Kupiainen A and Saksman E, 2009 arXiv:0909.1003
- [9] Bacry E, Delour J and Muzy J F, 2001 *Phys. Rev. E* **64** 026103
Schmitt F, 2003 *Eur. J. Phys. B* **34** 85
- [10] Vargas V and Rhodes R, 2008 arXiv:0807.1036
- [11] Ostrovsky D, 2008 *Lett. Math. Phys.* **83** 265
- [12] Gyorgyi G, Moloney N R, Ozogany K and Racz Z, 2007 *Phys. Rev. E* **75** 021123
Gyorgyi G, Moloney N R, Ozogany K and Racz Z, 2008 *Phys. Rev. Lett.* **100** 210601
- [13] Fyodorov Y V and Bouchaud J P, 2008 *J. Phys. A: Math. Theor.* **41** 372001
- [14] Faleiro E, Gómez J M G, Molina R A, Munoz L, Relano A and Retamosa J, 2004 *Phys. Rev. Lett.* **93** 244101
- [15] Bolthausen E, Deuschel J-D and Giacomin G, 2001 *Ann. Probab.* **29** 1670
Bolthausen E, Deuschel J-D and Zeitouni O, 1995 *Commun. Math. Phys.* **170** 417
Daviaud O, 2006 *Ann. Probab.* **34** 962
- [16] Derrida B, 1981 *Phys. Rev. B* **24** 2613
- [17] Derrida B and Spohn H, 1988 *J. Stat. Phys.* **51** 817
- [18] Mörters P and Ortgiese M, 2008 *J. Math. Phys.* **49** 125203
- [19] Fyodorov Y V and Bouchaud J P, 2008 *J. Phys. A: Math. Theor.* **41** 324009
Fyodorov Y V and Sommers H-J, 2007 *Nucl. Phys. B* **764** 128
- [20] Forrester P J and Warnaar S O, *Bull. Am. Math. Soc.* **45** 489
- [21] Adamchik V S, *On the Barnes function*, 2001 *Proc. 2001 Int. Symp. on Symbolic and Algebraic Computation (London, July)* (New York: Academic) pp 15–20
- [22] Gradshteyn I S and Ryzhik I M, 2000 *Table of Integrals, Series, and Products* 6th edn (New York: Academic) p 668 Eq. 6.561.16
- [23] Fateev V, Zamolodchikov A and Zamolodchikov A, 2000 arXiv:hep-th/0001012
- [24] Joanny J F and De Gennes P G, 1984 *J. Chem. Phys.* **81** 552
- [25] Bottcher A and Grudsky S, 2005 *Spectral Properties of Banded Toeplitz Matrices* (Philadelphia: SIAM)
- [26] Ostrovsky D, 2009 *Commun. Math. Phys.* **288** 287